Injectable liposomal docosahexaenoic acid alleviates atherosclerosis progression and enhances plaque stability

Suet Yen Chong [a,b,c], Xiaoyuan Wang [a,b], Louis van Bloois [d], Chenyuan Huang [a,b,c], Nilofer Sayed Syeda [a,c], Sitong Zhang [a,c], Hui Jun Ting [a,b,c], Vaarsha Nair [a,c], Yuanzhe Lin [e], Charles Kang Liang Lou [a,c], Ayca Altay Benetti [f], Xiaodong Yu [a,c], Nicole Jia Ying Lim [g], Michelle Siying Tan [a,c], Hwee Ying Lim [h,i], Sheau Yng Lim [h,i], Chung Hwee Thiam [h,i], Wen Donq Looi [j], Olga Zharkova [a,b], Nicholas W.S. Chew [g,k], Cheng Han Ng [g], Glenn Kunnath Bonney [a,l], Mark Muthiah [g,m,n], Xiaoyuan Chen [a,c,o,p,q], Giorgia Pastorin [f], A. Mark Richards [b], Veronique Angeli [h,i], Gert Storm [a,c,d,r,*], Jiong-Wei Wang [a,b,c,s,*]

[a] Department of Surgery, Yong Loo Lin School of Medicine, National University of Singapore, 119228 Singapore, Singapore
[b] Cardiovascular Research Institute, Yong Loo Lin School of Medicine, National University of Singapore, 117599 Singapore, Singapore
[c] Nanomedicine Translational Research Programme, Centre for NanoMedicine, Yong Loo Lin School of Medicine, National University of Singapore, 117609 Singapore, Singapore
[d] Department of Pharmaceutics, Faculty of Science, Utrecht University, 3584 CG Utrecht, the Netherlands
[e] Department of Biomedical Engineering, National University of Singapore, 117583 Singapore, Singapore
[f] Department of Pharmacy, Faculty of Science, National University of Singapore, 117543 Singapore, Singapore
[g] Yong Loo Lin School of Medicine, National University of Singapore, 117599 Singapore, Singapore
[h] Immunology Translational Research Programme, Department of Microbiology and Immunology, Yong Loo Lin School of Medicine, National University of Singapore, 117456 Singapore, Singapore
[i] Immunology Programme, Life Sciences Institute, National University of Singapore, 117456 Singapore, Singapore
[j] Bruker Daltonics, Bruker Singapore Pte. Ltd., 138671 Singapore, Singapore
[k] Department of Cardiology, National University Heart Centre, National University Hospital, 119074 Singapore, Singapore
[l] Division of Hepatobiliary and Pancreatic Surgery, Department of Surgery, National University Hospital, 119074 Singapore, Singapore
[m] Division of Gastroenterology and Hepatology, Department of Medicine, National University Hospital, 119074 Singapore, Singapore
[n] National University Centre for Organ Transplantation, National University Health System, 119074 Singapore, Singapore
[o] Department of Diagnostic Radiology, Yong Loo Lin School of Medicine, National University of Singapore, 119074 Singapore, Singapore
[p] Departments of Chemical and Biomolecular Engineering, and Biomedical Engineering, Faculty of Engineering, National University of Singapore, 117575 Singapore, Singapore
[q] Clinical Imaging Research Centre, Centre for Translational Medicine, Yong Loo Lin School of Medicine, National University of Singapore, 117599 Singapore, Singapore
[r] Department of Biomaterials, Science and Technology, Faculty of Science and Technology, University of Twente, 7522 NB Enschede, the Netherlands
[s] Department of Physiology, National University of Singapore, 117593 Singapore, Singapore

ARTICLE INFO

ABSTRACT

Atherosclerosis is a chronic inflammatory vascular disease that is characterized by the accumulation of lipids and immune cells in plaques built up inside artery walls. Docosahexaenoic acid (DHA, 22:6n-3), an omega-3 poly-unsaturated fatty acid (PUFA), which exerts anti-inflammatory and antioxidant properties, has long been purported to be of therapeutic benefit to atherosclerosis patients. However, large clinical trials have yielded inconsistent data, likely due to variations in the formulation, dosage, and bioavailability of DHA following oral intake. To fully exploit its potential therapeutic effects, we have developed an injectable liposomal DHA formulation intended for intravenous administration as a plaque-targeted nanomedicine. The liposomal formulation protects DHA against chemical degradation and increases its local concentration within atherosclerotic lesions. Mechanistically, DHA liposomes are readily phagocytosed by activated macrophages, exert potent anti-inflammatory and antioxidant effects, and inhibit foam cell formation. Upon intravenous administration, DHA liposomes accumulate preferentially in atherosclerotic lesional macrophages and promote polarization of

---

* Corresponding authors at: Department of Surgery, Yong Loo Lin School of Medicine, National University of Singapore, 119228 Singapore, Singapore.
E-mail addresses: g.storm@uu.nl (G. Storm), surwang@nus.edu.sg (J.-W. Wang).

macrophages towards an anti-inflammatory M2 phenotype, resulting in attenuation of atherosclerosis progression in both ApoE$^{-/-}$ and Ldlr$^{-/-}$ experimental models. Plaque composition analysis demonstrates that liposomal DHA inhibits macrophage infiltration, reduces lipid deposition, and increases collagen content, thus improving the stability of atherosclerotic plaques against rupture. Matrix-assisted laser desorption/ionization mass spectrometry imaging (MALDI-MSI) further reveals that DHA liposomes can partly restore the complex lipid profile of the plaques to that of early-stage plaques. In conclusion, DHA liposomes offer a promising approach for applying DHA to stabilize atherosclerotic plaques and attenuate atherosclerosis progression, thereby preventing atherosclerosis-related cardiovascular events.

1. Introduction

Atherosclerosis is a chronic inflammatory vascular disease which is estimated to account for 85% of cardiovascular disease (CVD) deaths annually [1]. The hallmark of atherosclerosis is the build-up of plaques within the intima layer of the artery walls. These atherosclerotic plaques mainly consist of lipids, inflammatory cells, smooth muscle cells, collagen fibres and cell debris [2]. Evidence from human and animal studies indicates that inflammation plays a critical role across all stages of atherosclerosis, including the initiation, development and destabilization of plaques [3,4]. Plaque rupture, an event accounting for 55–65% of coronary thrombi, is also highly associated with the inflammatory status and composition of atherosclerotic plaques [5]. Of note, recent findings in large lipid-lowering clinical trials show that chronic inflammation in high-risk atherosclerosis patients (with a plasma level of high sensitive C-reactive protein (hsCRP) $\geq$ 2 mg/L) remains at increased CVD risk despite having optimal or statin-controlled plasma levels of low-density lipoprotein cholesterol (LDLC <70 mg/dL) [6–8]. Such patients, who are on intensive statin therapy, are classified as having residual inflammatory risk which is common in lipid-lowering trials with approximately 43 to 47% reported to have elevated levels of hsCRP. Such high-risk patients would benefit from an additional therapeutic approach targeting plaque inflammation rather than lipid metabolic pathways [9]. In fact, inhibition of pro-inflammatory pathways such as NLPR3, IL-1β or NF-κB signalling pathways has been reported to reduce atherogenesis in mouse models [10,11]. Clinically, as reported in the CANTOS clinical trial (NCT01327846), the IL-1β monoclonal antibody Canakinumab reduces secondary cardiovascular events irrespective of the blood lipid levels [12]. Furthermore, the use of colchicine (an anti-inflammatory, immune-modulating drug normally prescribed for gout) has been recently shown to reduce major adverse cardiovascular events in patients who suffered from a recent myocardial infarction [13]. These clinical trials confirm the clinical value of anti-inflammatory therapies in atherosclerotic cardiovascular diseases.

Docosahexaenoic acid (DHA, 22:6n-3) is an omega-3 polyunsaturated fatty acid (PUFA) found primarily in cold-water fish such as salmon and tuna and is claimed to be of benefit for patients with CVD [14–18]. It is a bioactive molecule which has potent anti-inflammatory, antioxidant, and antiproliferative properties [19–24]. Additionally, it is a natural endogenous ligand for peroxisome proliferator-activated receptors. Activation of these receptors by DHA enhances fatty acid β-oxidation in the mitochondria, leading to an increase in fatty acid catabolism and subsequent reduction of triglyceride levels in the plasma [25,26]. The use of DHA (together with eicosapentaenoic acid) has been recommended in clinical guidelines for the treatment of persistently elevated severe hypertriglyceridemia [27–29]. Eicosapentaenoic acid (EPA) is also an omega-3 PUFA that exerts cardioprotective effects and has interlinked metabolism with DHA [30]. However, DHA and EPA are structurally distinct molecules with different biological effects, chemical stability, and secondary metabolites [30,31]. As DHA is partly converted into EPA *in vivo*, oral supplementation with DHA increases blood and tissue levels of both DHA and EPA in preclinical as well as clinical studies [32–36]. Interestingly, supplementation with DHA induces a higher increase in the Omega-3 Index (an index calculated based on the levels of EPA and DHA in red blood cell membranes, which is inversely associated with the risk of

coronary heart disease and related mortality) than with EPA, indicating the greater potency of DHA to modulate CVD risk [37].

Nevertheless, the role of DHA in the primary prevention of coronary heart disease remains controversial due to the inconsistent results yielded from recent randomized controlled clinical trials [38–41]. These discrepancies are likely due to variations in bioavailability and bioactivities of DHA following oral administration as high blood levels of DHA are needed to achieve cardioprotective effects [40,42]. Indeed, most oral DHA supplements suffer from poor absorption by the gut particularly if taken without high-fat meals [43]. Additionally, poor chemical stability of DHA may have affected the bioactivities of DHA in oral supplements [44,45]. Due to the high degree of unsaturated fatty acids in DHA, it can be readily oxidized to fatty acid peroxides, alcohols, and aldehydes when exposed to oxygen, light or heat. Though the actual *in vivo* effects of oxidized DHA is still a matter of debate [46], some *in vitro* studies have demonstrated that oxidized DHA derivatives might have different pharmacological properties compared to intact DHA [47,48]. However, most clinical trials have failed to monitor and report DHA's oxidation levels, given the growing evidence that >50% of the over-the-counter omega-3 supplements have oxidation levels that exceeded the recommended guidelines [49,50]. Hence, to protect DHA against chemical degradation and fully exploit its potential therapeutic effects, we have developed a liposomal DHA formulation intended for intravenous administration for the treatment of high-risk atherosclerosis patients.

Usually, DHA is administered *via* oral supplements. In this paper, we focus on intravenous administration of DHA liposomes. Intravenous administration of omega-3 PUFA in the form of lipid emulsions is used as a form of parenteral nutrition for patients suffering from gastrointestinal cancer or critical illness for many years [51]. In several preclinical *in vivo* models of stroke and heart ischemia, i.v. infusion of DHA/triglyceride emulsions resulted in a reduced event risk. [52–54]. Our focus is on the therapeutic utility of liposomes as plaque-targeted carriers. Liposomes are one of the most established nano-drug delivery systems for targeted drug delivery and have been demonstrated to accumulate in infarcted myocardium in experimental animal models [55] and atherosclerotic plaque macrophages in humans [56]. Liposome accumulation can occur by virtue of the enhanced permeability of endothelial linings within the atherosclerotic plaques [57]. In case of intravenously administered DHA liposomes, the accumulation effect can result in increased local DHA levels, which may enable increased local bioactivity within plaques when compared to the administration of oral DHA supplements. In this study, we aimed to develop well-characterized DHA liposomes and to evaluate relevant biological activities and underlying mechanisms using *in vitro* cultured primary macrophages and two mouse models of atherosclerosis.

2. Materials and methods

2.1. Materials

1,2-Dipalmitoyl-*sn*-glycero-3-phosphocholine (DPPC), *N*-(carbonyl-methoxy- PEG2000)-1,2-distearoyl-*sn*-glycero-3-phosphoethanolamine (DSPE-PEG2000),1,2-distearoyl-*sn*-glycero-3-phosphoethanolamine-N-[amino (polyethylene glycol)–2000]-N-(Cyanine 5) (DSPE-PEG2000-N-Cy5), L-α-Phosphatidylethanolamine-N-(lissamine rhodamine B sulfonyl) (Rhodamine-PE), cholesterol, docosahexaenoic acid (DHA),

chloroform, methanol, 4-(2-hydroxyethyl)- 1-piperazineethanesulfonic acid (HEPES)-buffered saline (HBS) solution (pH 7.4), arachidonic acid, lipopolysaccharides (LPS), interferon-γ (IFN- γ) and interleukin-4 (IL-4) were all purchased from Merck KGaA (Darmstadt, Germany). Dulbecco's Modified Eagle Medium (DMEM) with high glucose, ACK lysis buffer, heat-inactivated fetal bovine serum (FBS), human oxidized low-density lipoprotein conjugated to Dil (Dil-OxLDL), human oxidized low-density lipoprotein (OxLDL), and macrophage colony-stimulating factor (M-CSF) were all purchased from Thermo Fisher Scientific (Massachusetts, United States).

2.2. Animals and experimental models of atherosclerosis

C57BL/6 J wild-type (WT) mice were purchased from InVivos (Singapore); female apolipoprotein E deficient mice (ApoE$^{-/-}$) and LDL receptor-deficient mice (Ldlr$^{-/-}$) were purchased from Jackson Laboratory (Maine, USA). All mice were housed under specific pathogen-free conditions with a 12/12-h light-dark cycle (lights on at 7 AM, lights off at 7 PM) at the Comparative Medicine Animal Vivarium at the National University of Singapore. WT mice were fed with standard chow diet while ApoE$^{-/-}$ and Ldlr$^{-/-}$ mice were given high-fat diet (HFD, 42% from fat, TD.88137, Envigo) to accelerate the development of atherosclerosis. All studies were approved by the National University of Singapore Institutional Animal Care and Use Committee (IACUC; animal protocol number: R17–1085 and R21–1032) and conformed to the guidelines on the care and use of animals for scientific purposes (NACLAR, Singapore, 2004) and the Guide for the Care and Use of Laboratory Animals published by the US National Institutes of Health (NIIH Publication, 8th Edition, 2011).

2.3. Preparation of liposomes

Control and DHA liposomes were prepared using the thin-film hydration method with DPPC, cholesterol, DSPE-PEG2000, and DHA (for DHA liposomes only) in molar ratios of 1.85:1:0.15:0 and 0.85:1:0.15:1, respectively [58]. Cy5 or Rhodamine-PE was added at 1 mol% for fluorescent labelling when applicable. Briefly, DPPC, cholesterol, DSPE-PEG2000 and DHA (for DHA liposomes only) were dissolved in chloroform-methanol (1:1 *v*/v, total 0.8 ml) in a 10 ml round-bottom flask. A lipid thin film was prepared by rotary evaporation (Büchi Labortechnik AG, Flawil, Switzerland), followed by an additional drying step under a stream of nitrogen for 1 h. The lipid film was hydrated with 1 ml HBS solution (pH 7.4) to form a lipid dispersion containing 80 mM total lipid (TL) and 21 μM of DHA. To downsize and form uniform-sized liposomes, the lipid dispersion was subjected to multiple sequential extrusion steps using a mini extruder (Northern Lipids, Burnaby, BC, Canada) through polycarbonate membranes (Avanti Polar Lipids, Inc., Alabama, United States) with final filters of pore size 100 nm. The resulting liposomes were centrifuged at 8000 ×*g* for 20 min. The supernatant was collected and centrifuged again at 15,000 ×*g* for 20 min. The liposomes were collected and filtered through a 0.22 μm nylon filter (Sartorius AG, Göttingen, Germany) before use.

2.4. Characterization of liposomes

The mean particle-size distribution, polydispersity index (PDI) and zeta-potential of the liposomes were determined by Zetasizer Ultra (Malvern Panalytical, UK). Liposomes were diluted 100 times in Milli-Q water before measurements. Liposome colloidal stability under storage conditions was studied by monitoring their mean size and size distribution every 4–5 days for 30 days upon storage in HBS at 4 °C. To determine the concentration of DHA in liposomes, DHA was extracted from DHA liposomes with methanol and measured by LC-MS/MS using an Acquity UPLC BEH C18 column (1.7 μm, 2.1 × 100 mm) in ESI negative mode on an Agilent 1290 Infinity ultra-high pressure liquid chromatography (UHPLC) system, coupled to an AB SCIEX QTRAP 5500 tandem mass spectrometry. Non-encapsulated DHA was removed by filter centrifugation of liposomes at 4000 rpm for 10 min with Amicon Ultra 100 kDa filter centrifuge tubes (MerckMillipore, Burlington, MA, USA). The encapsulation efficiency was derived with the following formula:

$$\text{Encapsulation efficiency } (\%) = \frac{\text{Amount of DHA in liposomes}}{\text{Total amount of DHA used}} \times 100$$

Additionally, the morphology of liposomes was characterized by transmission electron microscope (TEM). Briefly, liposomes were fixed with 2.5% glutaraldehyde for 1 h at 4 °C. 20 μl sample was deposited onto a Formvar Film 200 mesh, CU, FF200-Cu grid for 15 min and was stained with 5% of gadolinium triacetate for 1 min. Images were then taken with transmission electron microscopy (FEI Tecnai G^2 Spirit with ICORR, Hillsboro, USA).

2.5. Stability of DHA

Freshly prepared DHA liposomes or DHA solubilized in cell culture medium (referred to as free DHA) were stored at 25 °C (room temperature, RT) or 4 °C, and sampled at several time-points to determine DHA concentrations by LC-MS/MS. 2 ml methanol was used to extract DHA from 20 μl of DHA liposomes or free DHA solution by sonicating at room temperature for 15 min. 0.1 μM arachidonic acid was spiked in the methanol as an internal standard. After centrifuging at 21,000 rpm for 10 min, the supernatant was collected for analysis. LC-MS/MS was performed using an Acquity UPLC BEH C18 column (1.7 μm, 2.1 × 100 mm) in ESI negative mode on an Agilent 1290 Infinity ultra-high pressure liquid chromatography (UHPLC) system, coupled to an AB SCIEX QTRAP 5500 tandem mass spectrometry. Eluent A consisted of 10 mM ammonium formate in Milli-Q water and eluent B consisted of 100% acetonitrile. Column and sample temperatures were set at 40 °C and 4 °C, respectively. Injection volume was set at 2 μl and flow was set at 0.45 ml/min. The eluent sequence and multiple reaction monitoring parameters, which were optimized for DHA and AA, were listed in Tables S1 and S2, respectively.

2.6. Cumulative drug release

In vitro cumulative release of DHA from liposomes was quantified using LC-MS/MS as described in Section 2.5. Briefly, freshly prepared DHA liposomes were diluted 10 times in PBS and transferred into a dialysis cassette (Slide A-Lyzer 10 k Dialysis Cassettes G2, #87731, Thermo Fisher Scientific, Massachusetts, United States) and immersed in 2000 ml of PBS (pH 7.4), used as a medium, in a 2 L beaker. The medium was stirred with a magnetic bar at 125 rpm and maintained at 37 °C. At predetermined time intervals (0, 0.5, 1, 3, 6, 10, 24, 48, and 72 h), the aliquots were withdrawn from the dialysis cassette. 1 ml of methanol was used to extract DHA from these aliquots. The cumulative release % for each time point was calculated based on the following equation:

$$\text{Cumulative release}\% = \frac{\text{Total encapsulated DHA - DHA recovered at specific time intervals}}{\text{Total encapsulated DHA}} \times 100$$

2.7. Preparation of bone marrow-derived macrophages

Bone marrow-derived macrophages (BMDM) were obtained by differentiating bone marrow cells collected from the femurs and tibias of WT mice as previously described [59–61]. Briefly, the bone marrow cells were cultured in Dulbecco's Modified Eagle Medium (DMEM) cell culture media supplemented with 20% heat-inactivated foetal bovine serum and 30 ng/ml macrophage colony-stimulating factor for 6 days in a humidified 5% CO_2 incubator at 37 °C. On day 7, cells were collected either used for flow cytometry analysis to confirm the macrophage lineage or seeded at the required density for other experiments. The list of antibodies was provided in Table S3. Data was acquired using a Fortessa flow cytometer (Beckman Coulter) and analysed with FlowJo (version 10.7.1). Macrophages were defined as $CD45^+/F4/80^+/CD11b^+/CD3^-/CD11c^-$, and Fluorescene minus one (FMO) was used as background control **(Fig. S10, Table S3)**.

2.8. In vitro assessment of DHA bioactivities

To determine bioactivities of DHA, 131 nM free DHA or DHA liposomes were added with LPS (100 ng/ml) and IFN-γ (20 ng/ml) to BMDM. After 4 h of incubation, cells were collected for RNA extraction. Total RNA was extracted with RNAeasy Mini Kit (Qiagen, Hilden, Germany) as per the manufacturer's protocol. Primers for inflammatory and antioxidant gene expression analysis used for RT-qPCR were listed in Table S4.

2.9. Cytotoxicity assay

PrestoBlue assay (A13262, Thermo Fisher Scientific, Massachusetts, United States) was used to assess the cytotoxicity of control liposomes, DHA liposomes and free DHA as per manufacturer's protocol. Briefly, BMDM were seeded in a 96-well plate overnight prior to treatment for 24 h with control liposomes, DHA liposomes, or free DHA, respectively. Cells were washed twice with PBS and incubated with PrestoBlue reagent diluted with pre-warmed complete-DMEM for 3 h at 37 °C in a humidified 5% CO_2 incubator. Then the fluorescence intensity was measured with a spectrophotometer.

2.10. Cellular uptake of DHA liposomes

The cellular uptake of DHA liposomes was conducted in a 12-well plate with either naive, M1, M2 or foam cell macrophages. M1 macrophages were induced by incubating BMDM with 100 ng/ml LPS and 20 ng/ml IFN-γ for 24 h. M2 macrophages were induced by incubating BMDM with 10 ng/ml IL-4 for 24 h. To generate foam cell macrophages, BMDM were stimulated with 100 ng/ml LPS and 20 ng/ml IFN-γ for 24 h followed by incubation with 80 μg/ml of oxidized low-density lipoprotein for 48 h. Cy5-labelled DHA liposomes (131 nM DHA) were then added to the cells in DMEM supplemented with 10% of heat-inactivated FBS. Cells were collected at various time points and stained for flow cytometry analysis or fluorescence microscopy (Nikon Eclipse Ti-E inverted microscope, Nikon Instrument Inc., Tokyo, Japan). Data was acquired using a Fortessa flow cytometer (Beckman Coulter) and analysed with FlowJo (version 10.7.1). M1 macrophages were defined as $CD45^+/F4/80^+/CD11b^+/iNOS^+/CD206^-$, M2 macrophages were defined as $CD45^+/F4/80^+/CD11b^+/iNOS^-/CD206^+$, foam cell macrophages were defined as $CD45^+/F4/80^+/CD11b^+/BODIPY^+$, and fluorescence minus one (FMO) was used as background control.

2.11. In vitro assessment of antioxidant activity

A cell permeable ROS indicator, $CM-H_2DCFDA$ (C6827, Thermo Fisher Scientific, Massachusetts, United States), was used to measure ROS production in BMDM. BMDM were seeded in a 12-well plate and pre-treated with control liposomes or DHA liposomes for 2 h before incubation with 100 ng/ml LPS and 20 ng/ml IFN-γ for 24 h. The cells were washed twice with PBS followed by staining with 10 μM $CM-H_2DCFDA$ in PBS for 45 min. Hoechst was used to stain cell nuclei. The fluorescence signal resulting from ROS production was captured with fluorescence microscopy. Data were presented as the percentage of ROS-positive cells over the total cell number.

2.12. Internalization of oxidized low-density lipoprotein

BMDM were seeded in a 96-well plate overnight prior to incubation with 100 ng/ml LPS and 20 ng/ml IFN-γ in serum-free DMEM for 24 h. Cells were then incubated with control or DHA liposomes for 2 h followed by incubation with Dil-labelled OxLDL (L34358, Thermo Fisher Scientific, Massachusetts, United States) at 40 μg/ml for 4 h. After washing with PBS, cells were fixed with 10% formalin, and stained with DAPI for cell nuclei. Images were taken with a fluorescence microscope (Nikon Eclipse Ti-E inverted microscope, Nikon Instrument Inc., Tokyo, Japan).

2.13. Foam cell formation

BMDM were seeded in a 96-well plate overnight prior to incubation with 100 ng/ml LPS and 20 ng/ml IFN-γ in serum-free DMEM for 24 h. Cells were then incubated with control or DHA liposomes for 2 h followed by incubation with Dil-labelled OxLDL (L34358, Thermo Fisher Scientific, Massachusetts, United States) at 80 μg/ml for 48 h. Cells were either washed twice with PBS and fixed with 10% formalin for Oil Red O (ORO) lipid staining or lysed with RLT lysis buffer for qPCR assay. The cell nuclei were counterstained with DAPI and haematoxylin. ORO staining was captured with both brightfield and fluorescent microscope.

2.14. Biodistribution study

Rhodamine-PE labelled DHA liposomes were injected intravenously into $ApoE^{-/-}$ mice (100 μl per mouse) which were fed on HFD for 8 weeks (to establish atherosclerotic plaques). Heart and whole aorta were harvested at 0 h, 2 h, 6 h and 24 h post-administration for *ex vivo* imaging with the IVIS Spectrum *in vivo* imaging system (Perkin Elmer, Waltham, Massachusetts, United States) as previously described [62]. In addition, the lungs, liver, spleen, and kidneys were also harvested at 24 h post-administration for *ex vivo* imaging. To localize the DHA liposomes within the atherosclerotic plaques, immunofluorescence staining (refer to 2.20 for detailed protocol) was performed on the cryosections of aortic root of $ApoE^{-/-}$ mice which received Cy5 labelled DHA liposomes. Cy5 fluorescent dye was used in this case as rhodamine-PE tends to photo-bleach during microscopy imaging.

2.15. Intervention study design

To evaluate the therapeutic efficacy of DHA liposomes in atherosclerosis, 4-week-old female $ApoE^{-/-}$ and $Ldlr^{-/-}$ mice were fed with HFD for 4 weeks, followed by 8 weeks intravenous administration of control liposomes or DHA liposomes (100 μl of 80 mM of total lipid, corresponding to 0.025 mg/kg of DHA; twice per week) while continuing HFD. At the endpoint, mice were euthanized with overdose isoflurane (5%). Blood was collected *via* cardiac puncture and stored in EDTA tubes for plasma preparation. Major organs including whole aorta, heart, brain, lungs, liver, spleen, and kidneys were isolated for further analysis.

2.16. Flow cytometry analysis of blood cells

Flow cytometry analysis of whole blood was performed as previously described [61]. Briefly, 50 μl of blood was collected *via* submandibular bleeding and stored in EDTA tubes. ACK lysis buffer was used to lyse the red blood cells and the white blood cells were collected by

centrifugation at 450 *g*, for 5 min. The supernatant was discarded, and the pellet was washed twice with staining buffer before staining with antibody cocktails. CD41 was used as a platelet marker, CD45 as a pan-leukocyte marker, Ly6G as a neutrophil marker, Ly6C as a monocyte marker, and CD11b as activation marker for neutrophils and monocytes. Neutrophils were defined as CD45$^+$ Ly6G$^+$; monocytes were defined as CD45$^+$ Ly6C^{high} for Ly6C high-expressing monocytes and CD45$^+$ Ly6C^{low} for Ly6C low-expressing monocytes. Fluorescence minus one (FMO) was used as the background control. Data was acquired using a Fortessa flow cytometer (Beckman Coulter) and analysed with FlowJo (version 10.7.1). The list of antibodies used for staining was provided in **Table S3**. The gating strategy was presented in **Fig. S7B**.

2.17. Analysis of plasma lipids and pro-inflammatory cytokines

Plasma was diluted 160 times in Biovision's sample dilution buffer to measure total cholesterol as per instructed by the Biovision total cholesterol fluorometric assay (Biovision, K603–100) user manual. Plasma total triglycerides was quantified using a triglyceride assay kit (ab65336, Abcam, Cambridge, United Kingdom) according to the manufacturer's instruction. Plasma levels of pro-inflammatory cytokines were determined with the Bio-Rad Pro Mouse Cytokine 23-plex assay (M60009RDPD, Bio-Rad, Hercules, California, United States).

2.18. Oil Red O staining of atherosclerotic plaques

The whole aorta was fixed in 10% formalin for 72 h and then incubated in 78% isopropanol for 5 min prior to staining with ORO working solution for 1 h on a rotating platform at room temperature. The aorta was washed twice with 78% isopropanol for 5 min and re-immersed in PBS. ORO-stained aorta was cut open longitudinally and pinned on a dissection plate with a dark background, then imaged with a stereo microscope (Nikon Instrument Inc., Tokyo, Japan) connected to a digital camera (Olympus DP22, Olympus Corporation, Tokyo, Japan). Images were analysed with ImageJ (version 1.53q 30 March 2022, NIH, DC, USA).

For aortic roots, cryosections were fixed in 10% formalin and washed once with PBS followed by incubation in ORO solution for 30 min. Tissue sections were rinsed twice in 60% isopropanol and washed with PBS for 5 min before being mounted with an aqueous-based mounting medium. Images were taken with a brightfield microscope (Nikon Eclipse Ti-E inverted microscope, Nikon Instrument Inc., Tokyo, Japan). Images were analysed with Nikon AR element analysis software version 4.5.0 (Nikon Instrument Inc., Tokyo, Japan) and presented as the percentage of total lesion area over total tissue area.

2.19. Matrix-assisted laser desorption/ionization mass spectra imaging

RapifleX (Bruker, MA, USA), a matrix-assisted laser desorption/ionization mass spectra imaging system (MALDI-MSI), was used to analyse the lipid profile in the aortic root. Harvested hearts were snap-frozen in liquid nitrogen and stored at −80 °C. 10 μm-thick cryosections of mouse aortic roots were mounted on conductive ITO slides (Bruker, MA, USA). Tissue sections were sprayed using the TM Sprayer M3 (HTX, North Carolina, United States) with a matrix solution containing 15 mg/ml of 2,5-dihydroxybenzoic acid dissolved in acetone nitrile/ddH$_2$O

(90/10) and 1% trifluoroacetic acid. Images were acquired in positive mode with 54% laser power, single mode, 1000 shots per pixel at 50 μm raster width. Mass spectrometry spectrums were re-aligned with calibrated endogenous lipid compounds. Data were processed and analysed in SCiLS Lab 2016b (Bruker, Massachusetts, United States) using linear discriminant analysis.

2.20. Immunofluorescence staining of aortic roots

Whole hearts were harvested and incubated in 10% formalin overnight then in 30% sucrose for 3 days at 4 °C. The heart was then embedded in the O.C.T compound and sectioned at 5 μm thick. Serial cryosections were collected when the first aortic cusp of the aortic root appeared. Aortic root sections were incubated with primary antibodies at 4 °C overnight followed by secondary antibodies conjugated to either Alexa-488 or Alexa-594. The list of antibodies used for staining is provided in Table S3. Pro-inflammatory M1 macrophages were identified as CD68 and iNOS double-stained cells while anti-inflammatory M2 macrophages were identified as CD68 and CD206 double-stained cells. Smooth muscle cells were stained with alpha smooth muscle actin (aSMA) antibody, while collagen type I antibody was used to determine collagen content in the plaques. All sections were mounted with anti-fade mounting medium containing DAPI (Vector Laboratories, California, United States). Images were captured with a fluorescent microscope and analysed with NIS-Element AR Analysis software version 4.5 (Nikon Instrument Inc., Tokyo, Japan).

2.21. Real-time quantitative polymerase chain reaction (RT-qPCR)

Total mRNA was isolated from fresh-frozen whole aorta with RNAeasy Mini Kit (Qiagen, Hilden, Germany) as per the manufacturer's protocol. 100 ng of total mRNA was converted to cDNA with QuantiTect Reverse Transcription Kit (Qiagen, Hilden, Germany) following the manufacturer's protocol. cDNA was mixed with PowerUp SYBR Green Master Mix (Thermo Fisher Scientific, Massachusetts, United States) and specific qPCR primers (listed in Table S4). mRNA expression levels were analysed with the QuantStudio 5 Real-Time PCR system (Thermo Fisher Scientific, Massachusetts, United States).

2.22. Statistical analysis

Statistical analysis was performed with GraphPad Prism 9 (version 9.3.1 GraphPad Software, California, USA). Data were presented as mean $\pm$ standard deviation (SD). Unpaired two-tailed *t*-test was performed for comparison of two groups and one-way analysis of variance (ANOVA) with Bonferroni's multiple comparisons was used for comparison of three groups or more. Statistical significance was annotated with * $p < 0.05$, ** $p < 0.01$, *** $p < 0.001$, **** $p < 0.0001$.

3. Results and discussion

3.1. Characteristics of DHA liposomes

The physicochemical characteristics of DHA liposomes are summarized in Table 1. Liposomes with the same lipid composition but not containing DHA were included as control. Both liposomes displayed

Table 1
Characteristics of DHA liposomes and control liposomes.

Liposomal formulation	Molar ratio (DPPC: Chol: DSPE-PEG$_{2000}$: DHA)	Freshly Prepared			After 30 days at 4 °C		
		Diameter (nm)	Poly-dispersity index	Zeta-potential (mV)	Diameter (nm)	Poly-dispersity index	Zeta-potential (mV)
DHA liposomes	0.85:1:0.15:1	127 ± 7	0.04 ± 0.03	−12 ± 6	125 ± 5	0.04 ± 0.01	−20 ± 4
Control liposomes	1.85:1:0.15:0	135 ± 11	0.04 ± 0.02	−16 ± 1	136 ± 11	0.02 ± 0.01	−18 ± 5

Data presented as mean $\pm$ SD of three independent liposome preparations.

comparable sizes around 130 nm with narrow size distribution as reflected by the low polydispersity indices (< 0.1). The colloidal stability of the liposomes at 4 °C was assessed over 30 days, with both formulations remaining stable regarding their size distribution (Table 1). The DHA encapsulation efficiency was 103 ± 4%, which corresponds to 21 μM of DHA and the drug loading efficiency was 18.4%. TEM analysis revealed that both liposomes were homogeneous nanospheres with a unilamellar phospholipid bilayer and an aqueous core typical of liposomal nanoparticles (Fig. S1A). Collectively, the encapsulation of DHA into the lipid bilayers did not alter the physicochemical properties of the liposomes. Additionally, the cumulative release profile of DHA from liposomes was investigated with a dialysis method at 37 °C in PBS solution. We observed a sustained release of DHA from liposomes within 48 h (Fig. S1B).

3.2. Protective effects of liposomal encapsulation of DHA on chemical stability and bioactivity

DHA is readily oxidized into hydroperoxides and aldehydes species upon exposure to oxygen in the air, light and heat [46]. We first assessed the chemical stability of free DHA upon storage at room temperature (RT) and 4 °C up to 28 days. Based on LC-MS/MS analysis, we observed that storage temperature has a significant impact on the chemical

stability of DHA. As evident from Fig. 1A, free DHA degraded much more rapidly when stored at RT compared to 4 °C. Chemical degradation is likely due to oxidation as the primary degradation process of DHA involves the reaction of molecular oxygen and free radicals with the polyunsaturated fatty acids [63]. 4-hydroxy-2-hexanal (4-HHE), 4-hydroxy-2-nonenal (4-HNE) and a wide variety of isoprostanes (which also serve as clinical markers of oxidative stress) are some common lipid peroxidation products of highly unsaturated fatty acids, including DHA and EPA [44]. The aim of the present study was not to identify the degradation products of DHA but rather to test if the degradation of DHA could affect its inherent bioactivities. Hence, we compared freshly prepared free DHA with free DHA which has been stored for 14 days at RT or 4 °C (as most DHA has been degraded at this time point (Fig. 1A).

One of the known bioactivities of DHA is its anti-inflammatory property involving the inhibition of the NF-kB signalling pathway through blocking of TLR4 dimerization and activation of the peroxisome proliferator-activated receptor (PPAR)-γ, resulting in reduced expression of NF-kB target genes such as TNF-α, IL-6 and IL-1β [64,65]. To investigate if any loss of chemical stability of DHA affects this anti-inflammatory property, we assessed the expression of pro-inflammatory genes, *i.e.*, CCL-2, TNF-α, IL-6, IL-1β, and iNOS, in M1-type inflammatory macrophages (see Materials & Methods) treated with free DHA prepared freshly or previously stored for 14 days at RT or
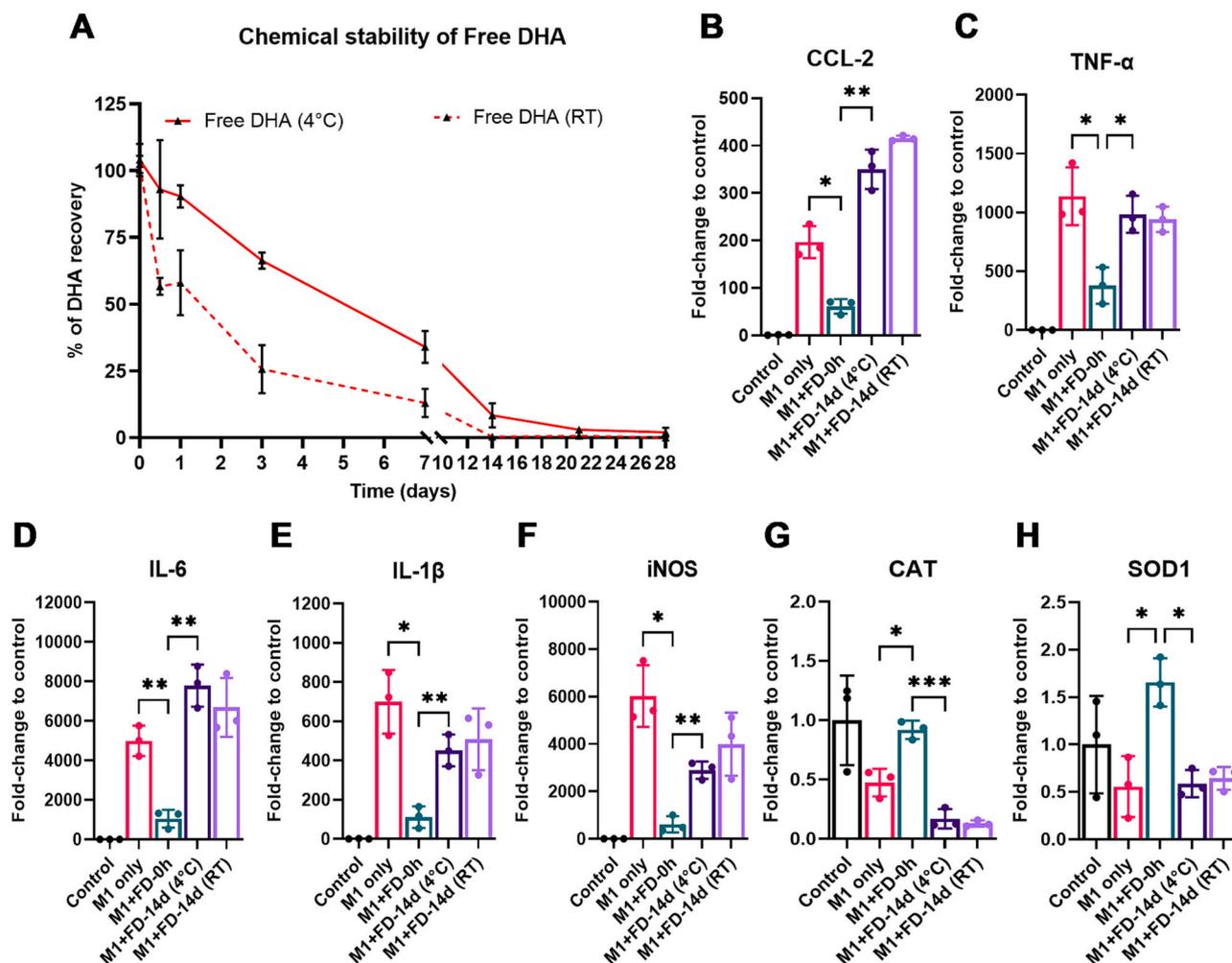
Fig. 1. Chemical stability and bioactivities of free DHA during storage. (A) Chemical stability of free DHA over 28 days when stored in dark at 4 °C or room temperature (RT). (B-H) Anti-inflammatory and antioxidant effects of free DHA on M1 macrophages. M1 macrophages were treated with freshly prepared (FD-0 h) or 14-day-old free DHA stored at 4 °C or RT [FD-14d (4 °C) or FD-14d (RT)]. Relative gene expression of pro-inflammatory cytokines and antioxidant enzymes were normalized against the housekeeping gene GAPDH and presented as fold changes compared with gene expression in naïve macrophages (Control). Data were expressed as mean ± standard deviation of three independent experiments; * $p < 0.05$, ** $p < 0.01$, *** $p < 0.001$, **** $p < 0.0001$.

4 °C. As shown in Fig. 1B – 1F, only freshly prepared free DHA (FD-0 h) was able to attenuate the inflammatory response in M1 macrophages as the expression levels of all the pro-inflammatory genes were lower when compared to untreated macrophages (M1) and macrophages treated with free DHA stored for 14 days at RT or 4 °C (FD-14d). No significant difference was observed between storage at RT or 4 °C. Additionally, DHA displays antioxidant activity *via* effects on mitochondrial functions and biogenesis [66]. Hence, we assessed the gene expression of the antioxidant enzymes catalase (CAT) and superoxide dismutase 1 (SOD1) as well. M1 macrophages have reduced gene expression of CAT and SOD1 as compared to unstimulated macrophages (Control). Freshly prepared free DHA was able to restore the gene expression of CAT and SOD1 to a similar level as in unstimulated macrophages (Control) whereas DHA stored for 14 days at RT or 4 °C did not (Fig. 1G & 1H). Collectively, free DHA lost anti-inflammatory and antioxidant bioactivities upon storage.

Many strategies have been employed to increase the chemical stability of DHA. The addition of antioxidant additives such as tocopherol, ascorbic acid, butylated hydroxyanisole (BHA), and butylated hydroxytoluene (BHT) is usually applied in oral DHA supplements. However, most of these additives are only allowed for oral delivery and some (synthetic BHA and BHT) can give rise to adverse side effects after oral

intake as reported in preclinical studies [67,68]. Here, we incorporated DHA into the phospholipid bilayers of liposomes and evaluated the chemical stability and bioactivities of DHA during storage in liposomal form. In terms of chemical stability, the liposomes could protect DHA from degradation for up to 28 days when stored at 4 °C (Fig. 2A). When stored at RT, we observed that the DHA only started to degrade on day 14 and continue to degrade gradually with >50% of DHA still detectable 28 days upon storage. The improved chemical stability of DHA is likely due to the protective phospholipid shield. Methods to assess the bioactivities of free DHA were also applied to DHA liposomes. As shown in Fig. 2B to 2F, freshly prepared and 14-day-old DHA liposomes which were stored at RT or 4 °C could reduce inflammatory responses in M1 macrophages by reducing the expression of the pro-inflammatory genes CCL-2, TNF-α, IL-6, IL-1β, and iNOS. Additionally, we observed a stronger anti-inflammatory effect of DHA liposomes than that with free DHA (Fig. 1). This effect is likely due to the higher intracellular uptake of DHA when encapsulated in liposomes which resulted in higher intracellular levels and activity of DHA. Additionally, gene expression of the antioxidant enzymes CAT and SOD1 were both increased in case of the DHA liposomes-treated cells (Fig. 2G & 2H). The antioxidant effect was preserved during storage of the DHA liposomes for 14 days at 4 °C and RT. Altogether, liposomal formulation of DHA protects DHA from
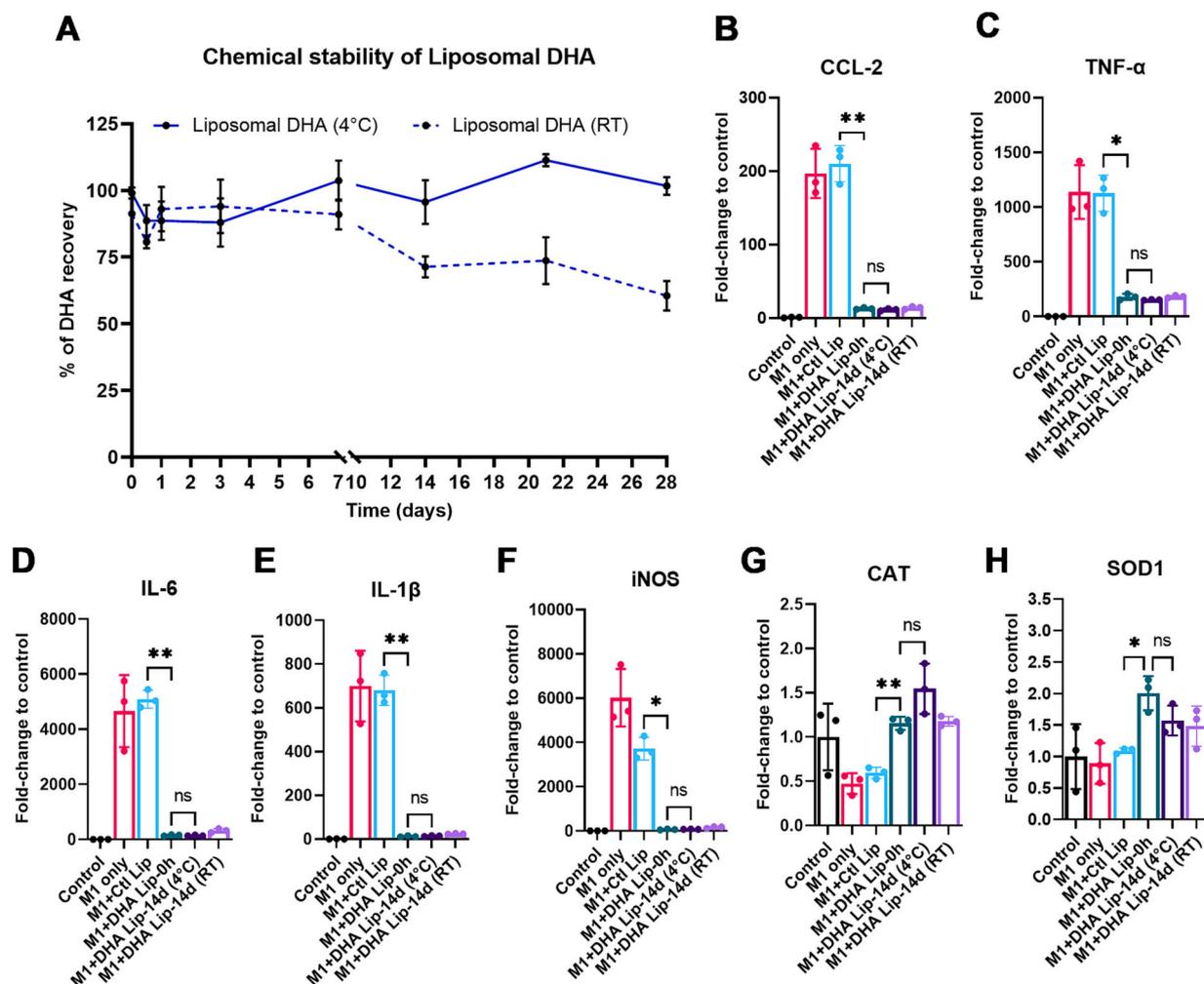
Fig. 2. Liposomal formulation protects DHA from chemical degradation and loss of bioactivity during storage. (A) Chemical stability of liposomal DHA over 28 days when stored in dark at 4 °C or room temperature (RT). (B-H) Anti-inflammatory and antioxidant effects of liposomal DHA on M1 macrophages. M1 macrophages were treated for 4 h with freshly prepared (DHA Lip-0 h) or 14-day-old liposomal DHA which were stored at 4 °C or RT [DHA Lip-14d (4 °C) or DHA Lip-14d (RT)]. Relative gene expression of pro-inflammatory cytokines and antioxidant enzymes were normalized against the housekeeping gene GAPDH and presented as fold changes compared with gene expression in naïve macrophages (Control). Data were expressed as mean ± standard deviation of three independent experiments; * $p <$ 0.05, ** $p < 0.01$, *** $p < 0.001$, **** $p < 0.0001$.

degradation and loss of bioactivities. From a chemical stability point of view, DHA liposomes can be stored for at least 4 weeks. Regarding the bioactivities, we showed that DHA preserved DHA stability for minimally 2 weeks. Nevertheless, in our experiments, freshly prepared liposomes were always used for *in vitro* and *in vivo* studies.

The products of lipid peroxidation of highly unsaturated fatty acids such as 4-hydroxy-2-hexenal (4-HHE) and 4-hydroxy-2-nonenal (4-HNE) are reported to be toxic [69,70]. Hence, we determined the potential cytotoxicity induced by the exposure of bone marrow-derived macrophages (BMDM) to DHA. DHA liposomes did not exert dose-dependent cytotoxicity, with no evidence of cell shrinkage and membrane blebbing (the morphological features of cell apoptosis) **(Fig. S2A & S2B)**. Hence, the encapsulation of DHA in liposomes may protect against the formation of cytotoxic degradation products.

3.3. DHA liposomes are readily taken up by activated macrophages

Monocyte-derived macrophages have been identified as the main driver of inflammation underlying the pathogenesis of atherosclerosis [71]. Pro-inflammatory M1 and foam cell macrophages are the predominant forms of macrophages found in atherosclerotic plaques [71]. Targeting and reducing the number of these subtypes of macrophages have been proven to be beneficial in treating atherosclerosis [72,73]. As liposomes preferentially target cells of the mononuclear phagocytic system (MPS), loading drugs into liposomes is one of the most widely used strategies to deliver drugs to these cells, especially tissue macrophages [74]. We assessed the cellular association of Cy5-labelled DHA liposomes by naïve (non-activated), M1 and M2 macrophages as well as foam cell macrophages (see Section 2.10). Bone marrow derived-macrophages (BMDM) were used in our study as it is known that they are more physiologically relevant than immortalized macrophage cell lines such as RAW 264.7 cells in terms of phagocytic activity, cytokine production and the regulation of oxidative burst during stimulation [75]. The degree of cellular association of DHA liposomes was time-dependent and affected by the phenotype of the macrophages (Fig. 3A). The cellular association of DHA liposomes was the lowest in case of naïve macrophages, with only 40% of Cy5 positive cells after 24 h. However, when the macrophages were activated to become M1, M2 or foam cell macrophages, approximately 80% of the cells became Cy5 positive. Based on the mean fluorescence intensity (MFI) of Cy5 (an indication of the association of DHA liposomes with the cells), M2 macrophages had the highest Cy5 signal after 24 h of incubation when compared to M1 and foam cell macrophages (Fig. 3A). These results were further verified with fluorescence imaging (Fig. 3B – 3E).This may be due to the activation-induced increase of protein corona-binding receptors- such as CD32, and CD36- on M2 macrophages, thereby enhancing the interaction with DHA liposomes [76]. Consistently, we observed an up-regulation of CD32 and CD36 gene expression in M2 macrophages when compared to control and M1 macrophages **(Fig. S3)**. The addition of serum proteins have reported to enhance the uptake of nanoparticles by M2 macrophages [76]. Collectively, DHA liposomes were taken up to a higher rate and extent by activated macrophages with the highest association with the M2 macrophages, followed by M1 macrophages, foam cell macrophages and naïve macrophages in a time-dependent manner.

3.4. DHA liposomes inhibit ROS production by M1 macrophages and polarise M1 macrophages to the M2 phenotype

Reactive oxygen species, metabolic by-products generated *via* the mitochondrial respiratory chain, play an important role in maintaining cellular homeostasis as they can serve as secondary messengers in different cell signalling pathways and cellular processes [77]. However, under pathological conditions, the balance of intracellular ROS is often perturbed, and excess ROS is produced leading to oxidative stress. In atherosclerosis, injured endothelial cells, M1 and foam cell macrophages

as well as activated smooth muscle cells generate excess ROS in response to vascular inflammation and injury, resulting in cellular apoptosis and tissue damage [78]. Accordingly, various nanomedicine strategies that use nanomaterials with antioxidant properties to scavenge ROS and reduce local inflammation have been proposed for the treatment of CVD [79]. In this study, we demonstrate that DHA liposomes possess antioxidant properties by increasing the gene expression of antioxidant enzymes such as CAT and SOD1 in M1 macrophages **(Fig. 2**G & 2**H)**. To further explore if the increased expression of antioxidant enzymes could reduce ROS in M1 macrophages, we assessed the ROS production in the M1 macrophages by an assay based on CM-H$_2$DCFDA, a general ROS indicator which emits green fluorescence upon the intracellular reaction with ROS. As shown in Fig. 4A**,** the ROS production in DHA liposomes-treated cells was significantly lower when compared to control liposomes-treated cells and untreated-M1 macrophages. This points to the antioxidant and ROS-scavenging properties of DHA liposomes.

Since ROS have been shown to be one of the factors which could facilitate the polarization of macrophages towards the M1 phenotype [80], we further assessed if the reduction of ROS by DHA liposomes could salvage M1 macrophages and promote the polarization of the M1 macrophages towards the M2 phenotype. After induction to M1 macrophages, DHA liposomes were added to the macrophages and incubated for 24 h. As demonstrated by FACS analysis, the percentage of M1 macrophages in the DHA liposomes-treated cells decreased drastically when compared to control liposomes (Fig. 4B & 4C). Additionally, the percentage of M2 macrophages increased in case of DHA liposomes-treated cells. Both effects resulted in lower M1/M2 macrophage ratios (Fig. 4B – 4E). Besides the potent antioxidant and anti-inflammatory effects of DHA, the increase in M2 macrophages is likely due to the pro-resolving properties of DHA's secondary metabolites, known as specialized pro-resolving mediators (SPMs). DHA-derived SPMs include protectins, D-series resolvins, and maresins which are generated enzymatically in the cell and are capable of polarizing macrophages into M2 phenotype [81]. To further investigate this, we incubated the M1 macrophages with DHA liposomes for a longer period (72 h). The percentage of M2 macrophages increased significantly to 11% for DHA liposomes-treated cells **(Fig. S4A & S4B)**. Consistently, we observed a decrease in the gene expression of M1 specific markers (CD40 and CD64) and an increase in the gene expression of M2 specific markers (CD206 and ARG1) in the DHA liposomes-treated cells when compared to control liposomes-treated cells **(Fig. S4C & S4D)**. Both CD40 and CD64 have been implicated in the pathogenesis of atherosclerosis. The down-regulation of these surface markers point to a reduced number of plaque M1 macrophages [82,83]. Contrary to M1 activation, M2 activation enhances arginase-1 activity and decreases ROS generation which helps in resolution of inflammation. Additionally, an increase in the number of M2 macrophages in the atherosclerotic plaques has also been associated with atherosclerosis regression, suggesting a beneficial role of the polarization of M1 macrophages to M2 phenotype for anti-atherosclerosis treatment [84].

3.5. DHA liposomes inhibit cellular uptake of OxLDL and foam cell formation

Intrusion and subsequent retention of oxidized LDL (OxLDL) into the vascular intima triggers the activation and transmigration of monocytes into the intima layer. As an attempt to clear the OxLDL from the extracellular space of the intima, the monocyte-derived macrophages phagocytose the OxLDL, leading to the formation of foam cell macrophages. Foam cell macrophages are pro-inflammatory and die easily due to the toxic effects of unesterified cholesterol derived from the OxLDL, contributing to the necrotic core of atherosclerotic plaques [85]. Hence, decreasing the formation of foam cells may be of therapeutic value in the context of atherosclerosis. After 4 h of incubation with OxLDL *in vitro*, approximately 40% of untreated M1 stimulated macrophages and control liposomes-treated M1 macrophages have taken up OxLDL, while
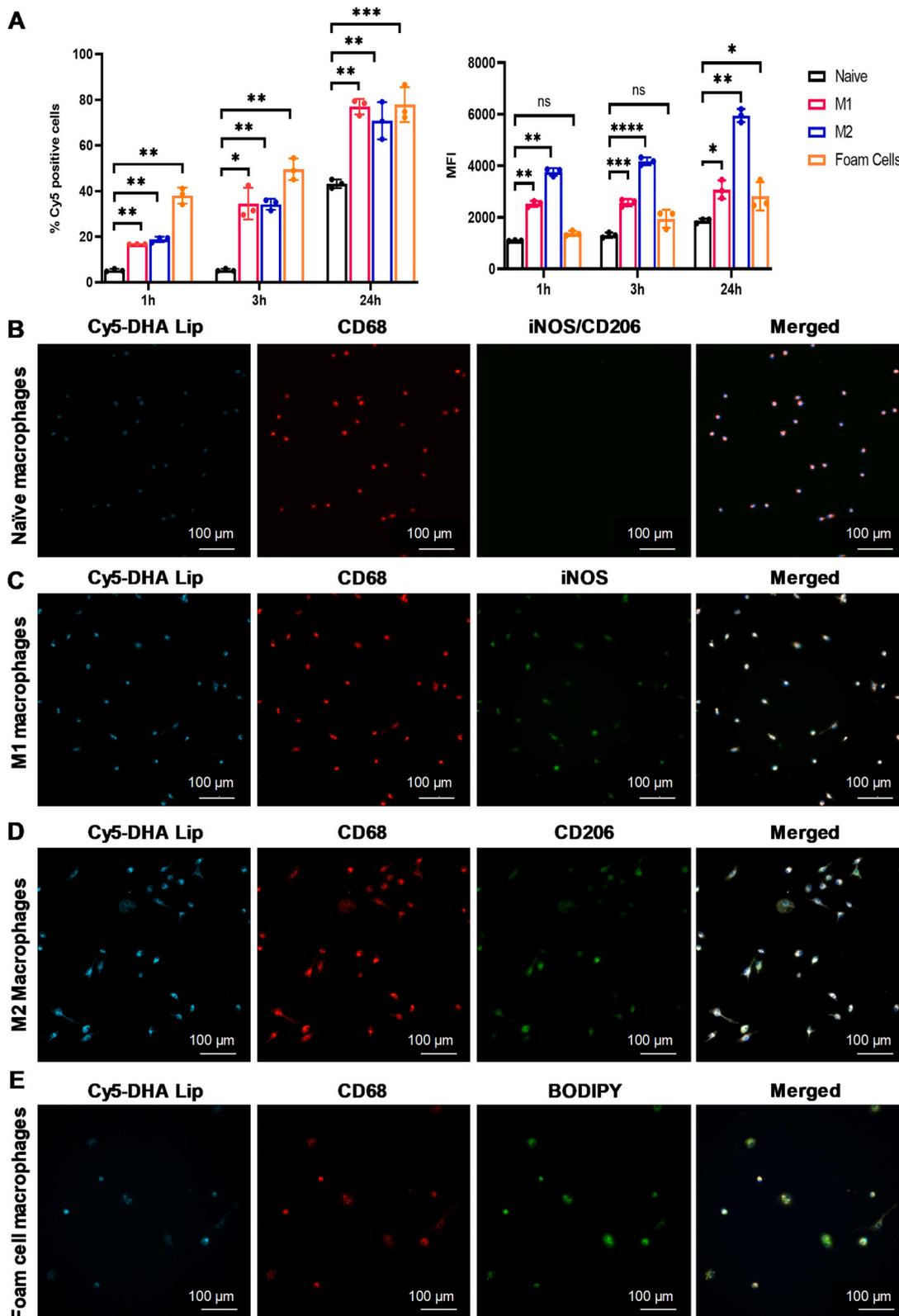
Fig. 3. DHA liposomes are taken up by activated macrophages. (A) Cells incubated with Cy5-labelled DHA liposomes for 1 h, 3 h or 24 h were analysed by flow cytometry. Cells taking up Cy5-labelled DHA liposomes were quantified by percentage of total cells or mean fluorescence intensity (MFI) in naïve, M1, M2, and foam cell macrophages. Data were expressed as mean ± standard deviation of three independent experiments; * $p < 0.05$, ** $p < 0.01$, *** $p < 0.001$, **** $p < 0.0001$. (B-E) Representative fluorescence microscopy images of naïve (CD68⁺ only), M1 (CD68⁺/iNOS⁺), M2 (CD68⁺/CD206⁺) and foam (CD68⁺/BODIPY⁺) macrophages after incubation with Cy5-labelled DHA liposomes for 24 h. Cell nuclei were stained with DAPI in blue. (For interpretation of the references to colour in this figure legend, the reader is referred to the web version of this article.)
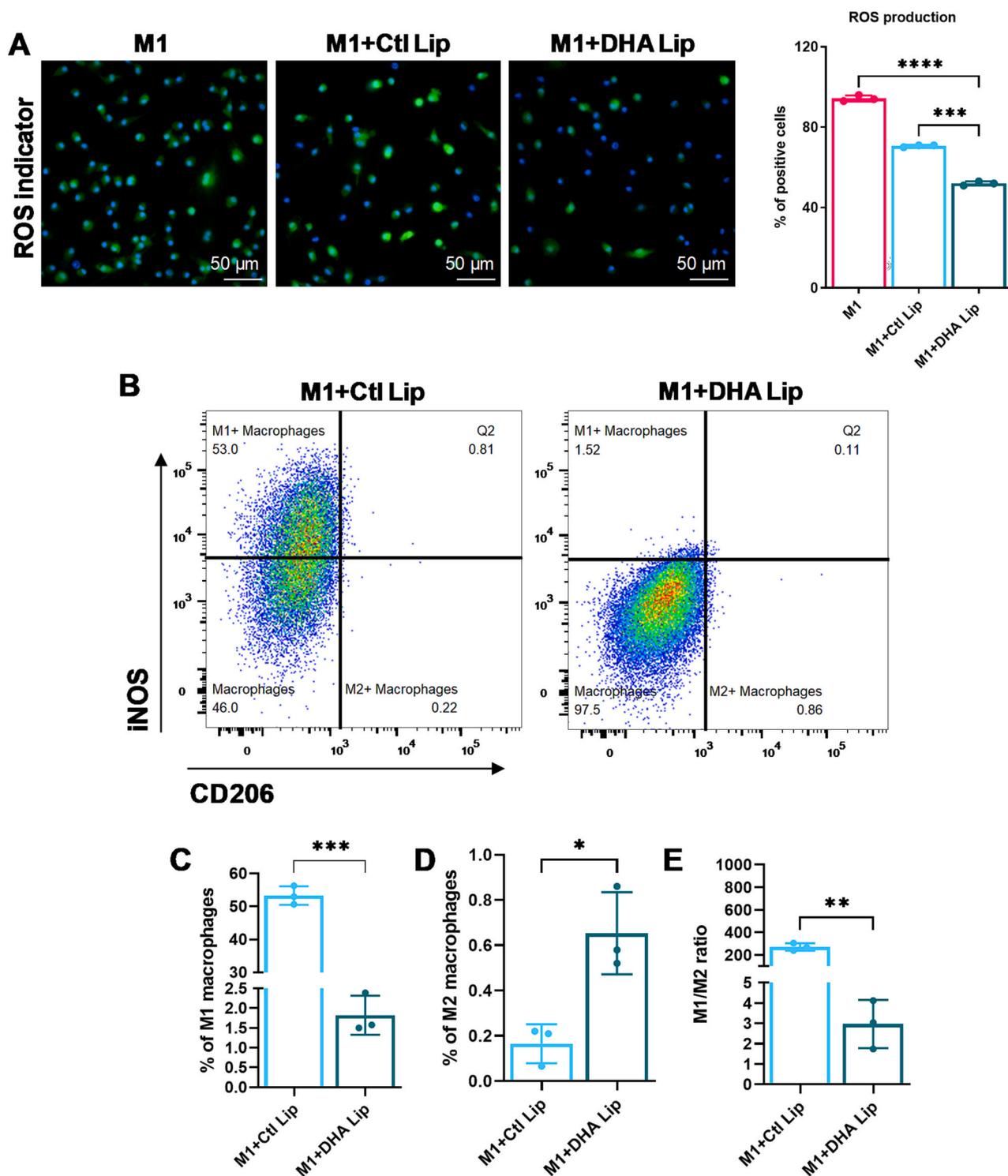
Fig. 4. DHA liposomes inhibit ROS production in M1 macrophages and promote polarization of M1 macrophages to the M2 phenotype. M1 macrophages were treated with control liposomes (Ctl Lip) or DHA liposomes (DHA Lip) for 24 h prior to further analysis. (A) Representative images of ROS production in M1 macrophages. Intracellular ROS was indicated in green and quantified for percentage of green fluorescence cells. Cell nuclei were stained with Hoechst in blue. Data were expressed as mean ± standard deviation of three independent experiments. (B) Representative flow cytometry scatter plots illustrating gating strategy for M1 and M2 macrophages. (C-E) Quantification of M1 and M2 macrophages and M1/M2 ratios based on flow cytometry analysis. Data were expressed as mean ± standard deviation of three independent experiments; * $p < 0.05$, ** $p < 0.01$, *** $p < 0.001$, **** $p < 0.0001$. (For interpretation of the references to colour in this figure legend, the reader is referred to the web version of this article.)
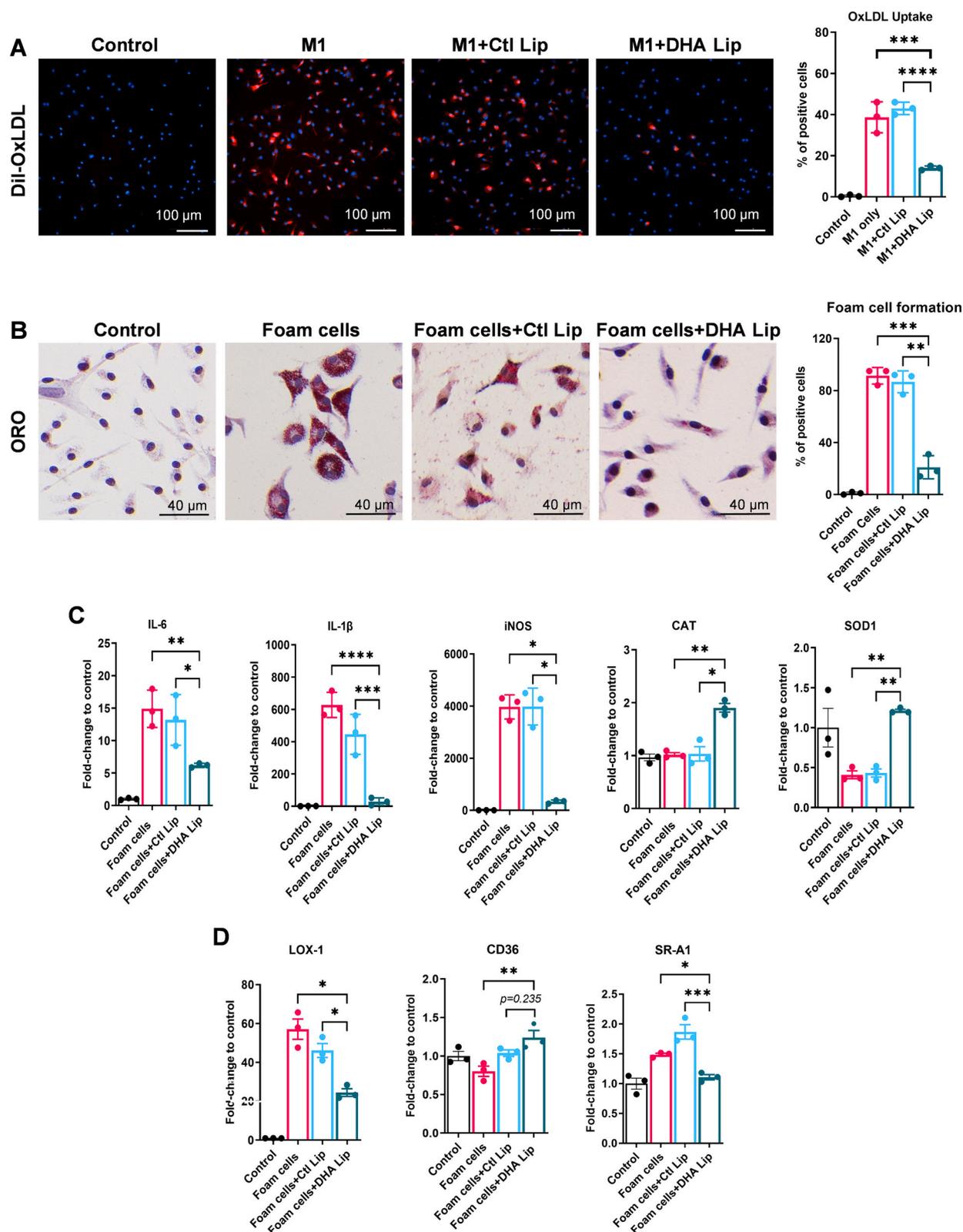
Fig. 5. DHA liposomes inhibit cellular uptake of OxLDL and foam cell formation. (A) Representative images of cellular uptake of OxLDL by M1 macrophages. Cell nuclei were stained with DAPI in blue and OxLDL in red. OxLDL-positive M1 macrophages were quantified as percentage of total cells (right panel). (B) Representative images of foam cells. Cell nuclei were stained with haematoxylin in purple and lipids were stained with ORO in red. Formation of foam cells was quantified as percentage of total cells (right panel). (C) Relative gene expression of pro-inflammatory cytokines (IL-6, IL-1β, and iNOS) and antioxidant enzymes (CAT and SOD1) in foam cells. (D) Relative gene expression of scavenger receptors (LOX-1, CD36 and SR-A1) in foam cells. Data were normalized against the housekeeping gene GAPDH and presented as fold changes of gene expression in naïve macrophages (Control). Data were expressed as mean ± standard deviation of three independent experiments; * $p < 0.05$, ** $p < 0.01$, *** $p < 0.001$, **** $p < 0.0001$. (For interpretation of the references to colour in this figure legend, the reader is referred to the web version of this article.)

only 14% of macrophages in case of the DHA liposomes-treated cells internalized OxLDL. Longer incubation of M1 macrophages with higher concentrations of OxLDL drove the macrophages into foam cells. Expectedly, in a period of 48 h, >80% of the macrophages converted into foam cells in the M1 stimulated and control liposomes-treated M1 cells, while DHA liposomes significantly inhibited foam cell formation to a level of only 20% (Fig. 5A & 5B). Gene expression analysis of foam cells revealed that DHA liposomes significantly decreased the expression of the pro-inflammatory cytokines IL-6, IL-1β, and iNOS (Fig. 5C). The gene expression of antioxidant enzymes CAT and SOD1 was increased in case of the DHA liposomes-treated cells (Fig. 5C). This shows that the anti-inflammatory and antioxidant properties of DHA-liposomes (Fig. 2B – 2H) are still present in case of OxLDL induced foam cell macrophages.

Lectin-like oxidized low-density receptor-1 (LOX-1), which is the main OxLDL receptor on endothelial cells, is also expressed on macrophages and upregulated in atherosclerosis pathology [86,87]. Indeed, the LOX-1 gene expression in the foam cells was increased. Treatment with DHA liposomes reduced expression of LOX-1 in the foam cells while control liposomes showed no effect (Fig. 5D). Scavenger receptors CD36 and SR-A1 in macrophages are implicated in atherogenesis [88,89]. Compared to control liposomes, DHA liposomes showed a trend to increase CD36 expression although the increase did not reach statistical significance (p-value = 0.235), indicating DHA liposomes may have mild effects on CD36 expression. In contrast, DHA liposomes markedly reduced the expression of SR-A1 in the foam cells compared to control liposomes (Fig. 5D). Lower expression of SR-A1 may contribute to reduced inflammation and less foam cell formation since SR-A1 was reported as a co-receptor of TLR4 involved in ER stress and macrophage apoptosis in atherosclerosis [90]. To sum up, our findings suggest that the attenuation in foam cell formation by DHA liposomes is attributed to the reduced expression of LOX-1 and SR-A1, and the resultant lower uptake of OxLDL by macrophages.

3.6. DHA liposomes accumulate in macrophages present in atherosclerotic plaques

Liposomes have been reported to localize in macrophages present in human atherosclerotic plaques upon intravenous injection [56]. Apart from the incorporation of DHA in the liposomal bilayers, the lipid composition of our liposomal DHA formulation was the same in case of the aforementioned liposomes. Therefore, we anticipated a similar pharmacokinetic performance of the intravenously administered DHA liposomes in atherosclerotic mice. As shown by IVIS imaging, DHA liposomes accumulated at the aortic arch and abdominal artery branching sites, resembling atherosclerosis-prone regions (Fig. 6A & 6B). Immunofluorescence staining and colocalization analysis revealed that the liposomes were taken up by macrophages in the plaques (Pearson's correlation coefficient = 0.945) (Fig. 6C & S5C). The accumulation of liposomes in the plaque is likely due to increased permeability along the endothelial linings caused by dysfunctional endothelium and enhanced angiogenesis in the vasa vasorum region [57]. Furthermore, the incorporation of polyethylene glycol (PEG) in the liposomes has increased the circulatory half-life of the liposomes and hence more liposomes could accumulate in the atherosclerotic plaques over time. Once inside the plaques, the liposomes were taken up by the macrophages *via* endocytosis [91]. Our *in vivo* findings are in line with our *in vitro* results showing higher association of DHA liposomes with activated macrophages such as M1, M2 and foam cell macrophages in a time-dependent manner (Fig. 3, **Fig. S5A & S5B**). Collectively, liposomal DHA can act as a carrier for DHA into plaque macrophages to enhance the beneficial effects of DHA to levels which are very unlikely to be achieved *via* oral supplementation due to low bioavailability.

3.7. DHA liposomes attenuate atherosclerosis in ApoE$^{-/-}$ and Ldlr$^{-/-}$ mice

Our *in vitro* assessment provided evidence that DHA liposomes are able to alleviate atherosclerosis through multiple mechanisms (Fig. 2 - 5). To evaluate anti-atherosclerotic effects of DHA liposomes *in vivo*, we utilized two atherogenic mouse models, apolipoprotein E deficient mice (ApoE$^{-/-}$) and LDL receptor deficient mice (Ldlr$^{-/-}$) (Fig. 7A). Although both models generate atherosclerotic plaques by feeding a high-fat diet (HFD), the features and underlying mechanism are different [92]. ApoE$^{-/-}$ mice are hyperlipidaemic and develop atherosclerotic plaques even when fed normal chow while Ldlr$^{-/-}$ mice only develop atherosclerosis when fed HFD [93]. If both ApoE$^{-/-}$ and Ldlr$^{-/-}$ mice are given the same duration of HFD, ApoE$^{-/-}$ mice will develop more atherosclerotic plaques of a more advanced stage than the Ldlr$^{-/-}$ mice. After 8 weeks of intravenous administration of 2 doses of DHA liposomes per week (in total 16 doses of 11 μg DHA each), there were significantly less atherosclerotic plaques formed in the aortic arch in case of the DHA liposomes-treated mice as compared to the control liposomes-treated mice in the ApoE$^{-/-}$ mouse model (Fig. 7B). Assessment of the "en face" lesion area in the whole aorta tree revealed that DHA liposomes were able to reduce the total lesional area by about 36% in ApoE$^{-/-}$mice and about 22% in Ldlr$^{-/-}$mice in comparison with control liposomes-treated mice (Fig. 7C & 7D). Clearly, DHA liposomes were able to attenuate the progression of atherosclerosis in both models. DHA has been reported to suppress atherogenesis in ApoE$^{-/-}$ mice previously [94–98]. However, the reported studies supplied DHA in HFD at the beginning of the study when the disease is not yet established. Whereas in our study, the atherosclerotic prone mice were given 4 weeks of HFD before the start of i.v. DHA liposomes treatment. Hence, our approach is to be considered as a therapeutic intervention rather than a preventive approach. In these studies, the amount of DHA given orally (ranging from 0.3 to 3 g/kg/day) was considerably higher when compared to our study (0.05 mg/kg/week), reflecting the potency of i.v. treatment with DHA liposomes.

To evaluate if DHA liposomes could affect the profile of different types of lipid species in the atherosclerotic plaques, we performed matrix-assisted laser desorption/ionization (MALDI) mass spectrometry imaging (MSI) on cryosections of these plaques (Fig. 7E). MALDI is a mass spectrometry technique used to ionize biomolecules such as DNA, proteins, peptides, and lipids which are fragile and tend to fragmentize when ionized by conventional ionization methods [99]. Furthermore, when applied on cryosections, MALDI can provide the spatial distribution of the target analytes. This technique has been applied to atherosclerotic plaques of animals as well as humans to dissect the spatial distribution of the complex lipid profiles in different stages of atherosclerotic plaque progression [100–103]. After 8 weeks of treatment with DHA liposomes, the aortic root of ApoE$^{-/-}$ mice was used for MALDI-MSI. ApoE$^{-/-}$ mice which were fed with HFD for the same duration but without any treatment (referred to as saline) were included as positive control while ApoE$^{-/-}$ mice which were fed with normal chow were used as healthy control. HE staining was performed on the same section after MALDI-MSI to demarcate the plaque area and co-register with the MALDI-MSI images for further analysis (Fig. 7E). The principal component analysis showed that the lipid profiles of the plaques of DHA liposomes-treated mice was similar to ApoE$^{-/-}$ mice fed with normal chow. In contrast, the lipid profiles of the plaques of control liposomes-treated mice were similar to those of untreated ApoE$^{-/-}$ mice fed with HFD, pointing to the need for DHA targeting to achieve this strong beneficial effect (Fig. 7F). ApoE$^{-/-}$ mice will develop atherosclerotic plaques even when fed with normal chow, but the disease progression will be slower and the plaques developed will be at an earlier stage [93]. HFD intensifies and accelerates atherogenesis in ApoE$^{-/-}$ mice. DHA liposomes are able to halt the progression of the plaques, preventing it from developing into advanced atherosclerotic plaques. This might be partly attributed to DHA liposomes' ability to
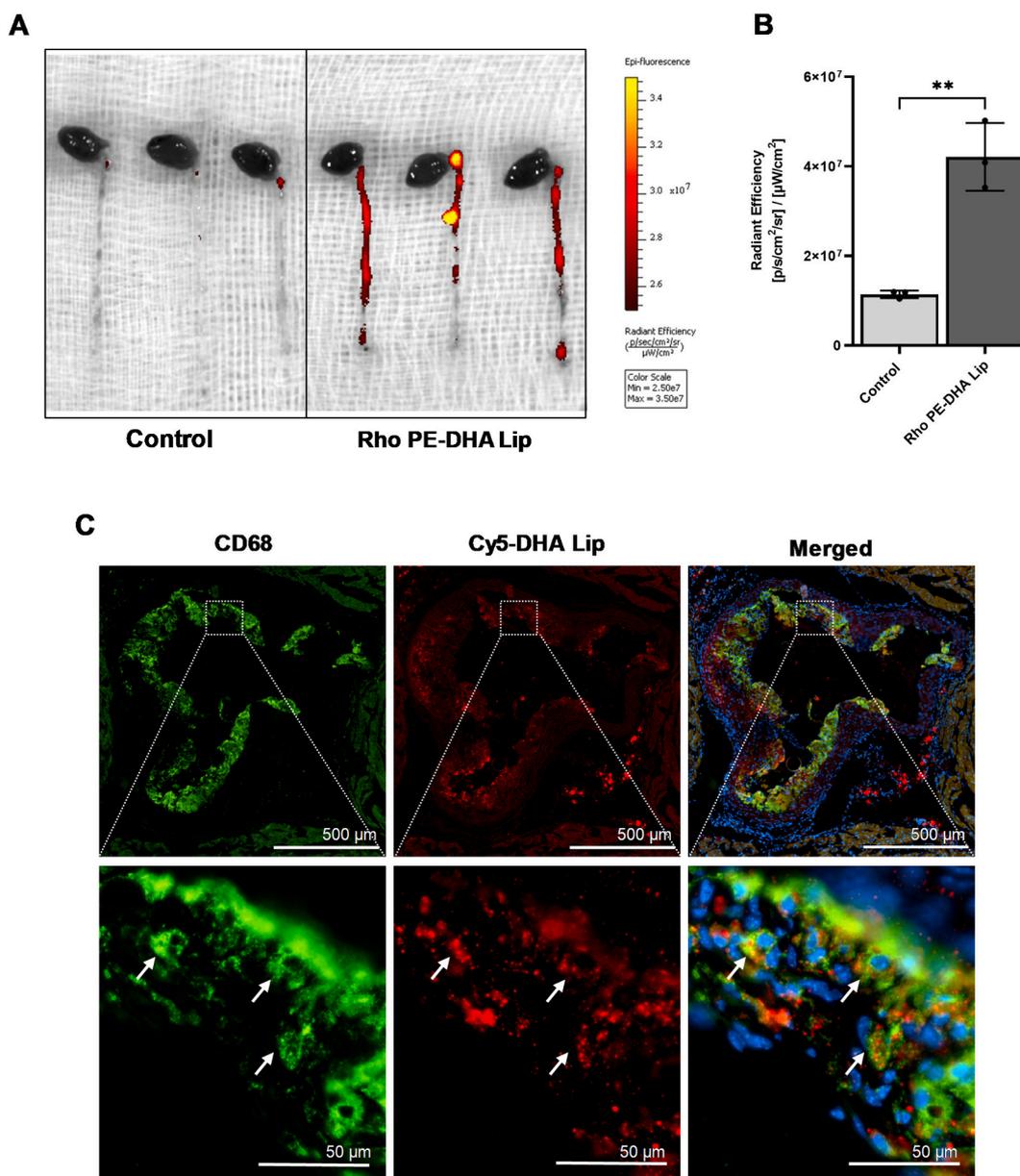
Fig. 6. DHA liposomes accumulate in macrophages of atherosclerotic plaques. (A) Representative *ex vivo* IVIS images of the hearts and whole aortas of ApoE$^{-/-}$ mice 24 h post-injection of unlabelled control liposomes (control; left) or rhodamine-PE labelled DHA liposomes (right). (B) Quantification of rhodamine-PE fluorescence signal in the aortas. $N = 3$ mice per group. Data were expressed as radiant efficiency and expressed as mean $\pm$ standard deviation; * $p < 0.05$, ** $p < 0.01$, *** $p < 0.001$. (C) Immunofluorescence staining of macrophages in the aortic root. ApoE$^{-/-}$ mouse aortas were collected 24 h post-injection of Cy5-labelled DHA liposomes. Cell nuclei were stained with DAPI in blue, macrophages were stained with CD68 in green, and DHA liposomes in red. Arrows indicate co-localization of DHA liposomes with macrophages. (For interpretation of the references to colour in this figure legend, the reader is referred to the web version of this article.)

inhibit OxLDL uptake and foam cell formation as shown in our *in vitro* data (Fig. 5). Indeed, early-stage plaques showed less lipid accumulation as compared to advanced atherosclerotic plaques [102]. Further investigation is warranted to identify and quantify the lipid species which are directly or indirectly affected by DHA liposomes.

To elucidate if the changes in lipid species in the plaques was related to changes in the blood lipid profile, we also measured plasma levels of total triglyceride (TG) and cholesterol (TC). No significant difference was observed in the TG and TC levels between the control liposomes and DHA liposomes treated mice (**Fig. S6A & S6B**). This data is consistent with some large clinical trials whereby DHA alone could not reduce plasma TG or TC [41].

To investigate if DHA liposomes could exert their anti-inflammatory effects systemically, we performed flow cytometry analysis on the blood cells of ApoE$^{-/-}$ mice before (Baseline) and after treatment (Post-

treatment) (**Fig. S7A & S7B**). DHA liposomes did not affect the number of systemic immune cells, including circulating neutrophils and monocyte subpopulations (Ly6C^{high} and Ly6C^{Low}) (**Fig. S7C – S7E**). There was no influence of DHA liposomes either on the formation of platelet-neutrophil complexes or platelet-monocyte complexes (**Fig. S7C – S7E**). In consistence, there was no difference in plasma levels of pro-inflammatory cytokines between control and DHA liposomes treated mice (**Fig. S8A & S8B**). Of note, consistent with previous report [104], HFD increased the expression of CD11b in the platelet-monocyte complexes (Fig. **S7D & S7E**), which was not affected by DHA liposome treatment. From these findings, we can deduce that DHA liposomes exert their anti-atherosclerotic effect locally in the plaques rather than systemically.
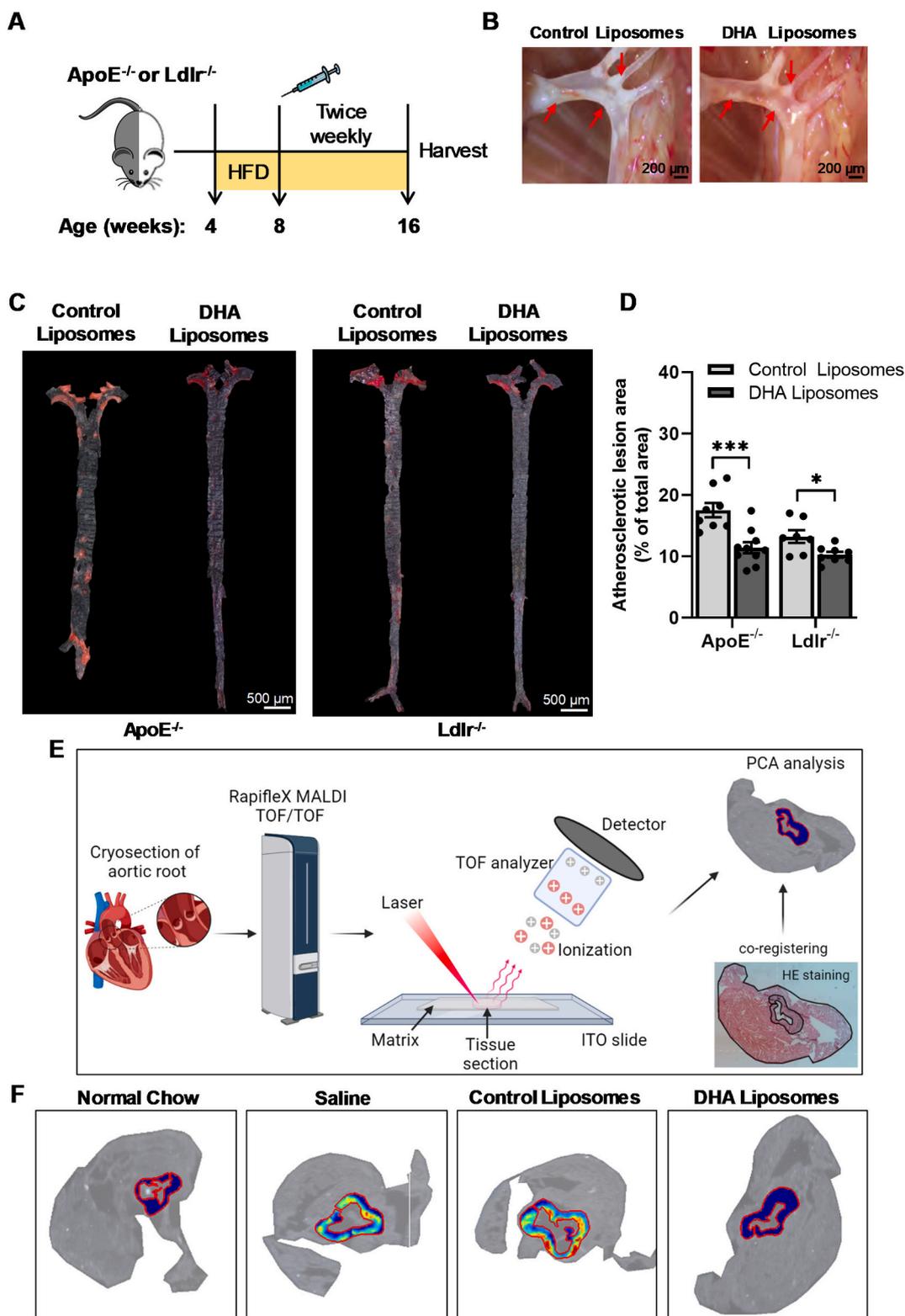
Fig. 7. DHA liposomes attenuate atherosclerosis in ApoE$^{-/-}$ and Ldlr$^{-/-}$ mice. (A) Schematic illustration of atherosclerotic mouse model development on high-fat diet (HFD) and the treatment schedule. (B) Representative images of aortic arch *in situ*. Arrows indicate the location of plaques. (C) Representative images of ORO-stained aortas. Plaques were stained red. (D) Quantification of atherosclerotic plaques. $N = 7$ to 10 mice per group. Data were expressed as mean $\pm$ standard deviation; * $p < 0.05$, ** $p < 0.01$, *** $p < 0.001$. (E) Schematic illustration of MALDI-MSI application on the cryosections of aortic root. The same section was stained with haematoxylin and eosin to co-register with the MALDI-MSI images for principal component analysis (PCA). The black lines demarcate different tissue regions. (F) Representative MALDI-MSI component images of aortic roots after PCA. The differences in the lipid profile of atherosclerotic plaques are denoted by the rainbow colour map. DHA liposome-treated mice exhibited a similar lipid profile with ApoE$^{-/-}$ mice that were fed on a normal chow diet, whereas control liposome-treated mice showed a similar lipid profile with ApoE$^{-/-}$ mice that were fed on HFD and injected with saline. (For interpretation of the references to colour in this figure legend, the reader is referred to the web version of this article.)
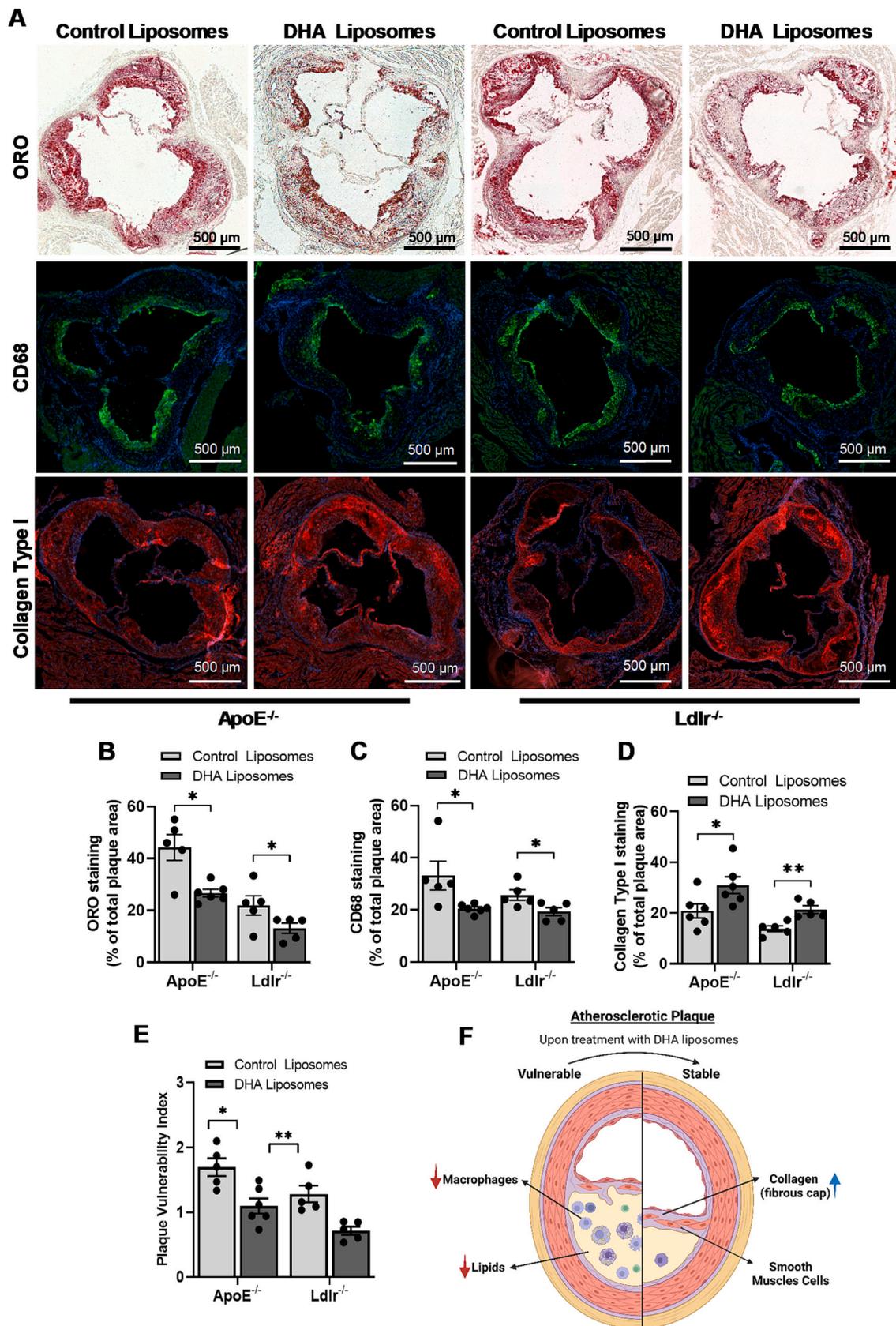
Fig. 8. DHA liposomes enhance plaque stability. (A) Representative images of lipid, macrophages and collagen staining used for quantification in panels B, C and D. (B-D) Quantification of lipid content (ORO staining), macrophage infiltration (CD68 immunofluorescence staining) and collagen fibres (collagen type I immuno-fluorescence staining) in atherosclerotic plaques. $N = 5$ to 6 mice per group. (E) Plaque vulnerability index (PVI) of mice subject to different treatments. N = 5 to 6 mice per group. Data were expressed as mean ± standard deviation; * $p < 0.05$, ** $p < 0.01$. (F) Schematic illustration of potential mechanisms *via* which liposomal DHA increases plaque stability.
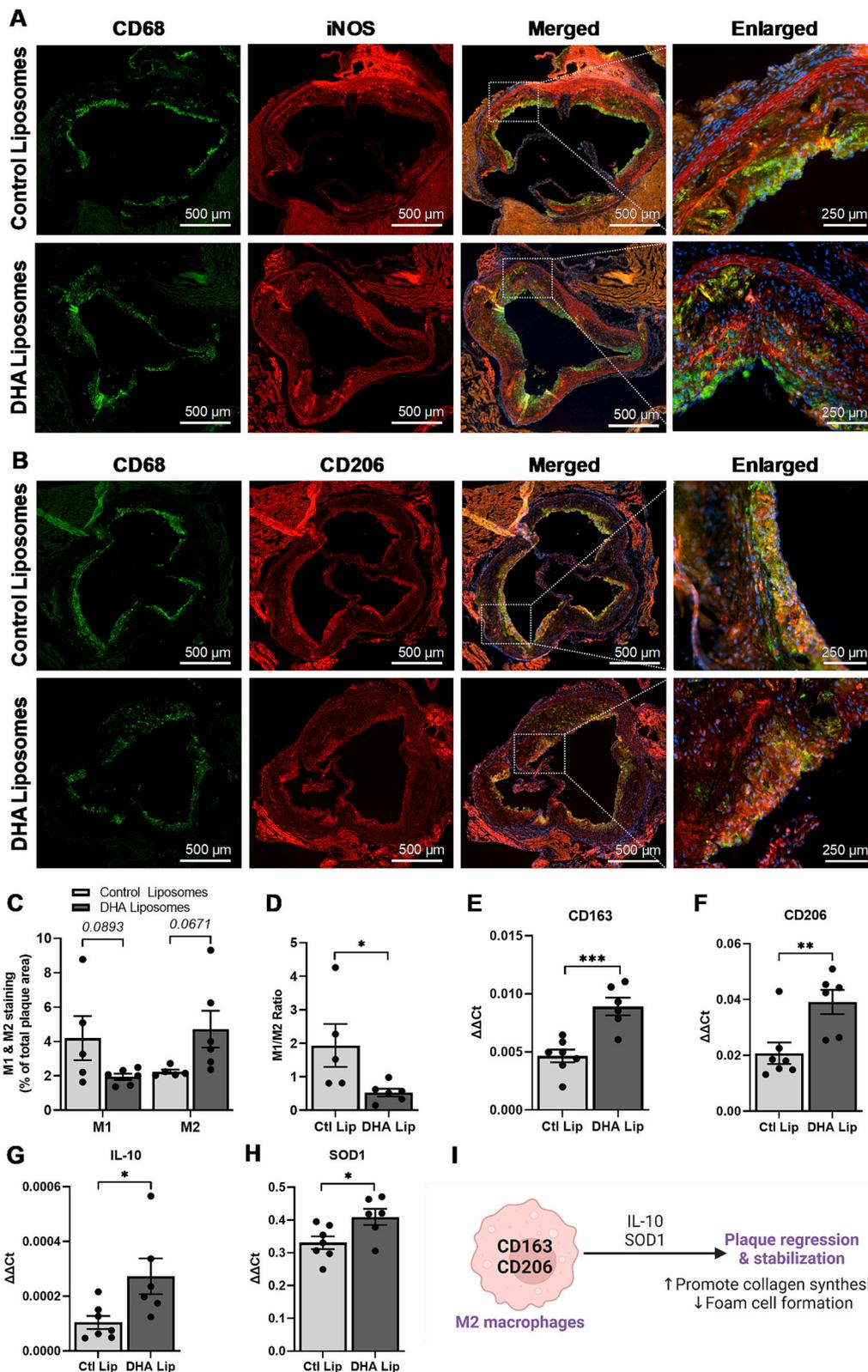
Fig. 9. DHA liposomes reduce pro-inflammatory M1 macrophages and increase reparative M2 macrophages in atherosclerotic plaques. (A and B) Representative images of aortic root sections stained for M1 (iNOS$^+$) and M2 (CD206$^+$) macrophages, respectively. Cell nuclei were stained with DAPI. Quantification of M1 and M2 macrophages (C) and ratios of M1 to M2 macrophages (D) in atherosclerotic plaques. N = 5 to 6 ApoE$^{-/-}$ mice per group. Gene expression of CD163 (E), CD206 (F), IL-10 (G), and SOD1 (H) in atherosclerotic aorta. $N = 6$ ApoE$^{-/-}$ mice per group. Data were expressed as mean $\pm$ standard deviation; * $p < 0.05$, ** $p < 0.01$. (I) Schematic diagram illustrating the hallmarks of M2 macrophages and potential pathways (anti-inflammation and antioxidant) that attenuate atherosclerosis progression.

3.8. DHA liposomes enhance plaque stability

Plaque rupture occurs when the fibrous cap fissures, initiating platelet aggregation at the opening site and increasing the risk for the formation of coronary thrombi which is the main cause of acute myocardial infarction or stroke. The chance for a rupture event is highly dependent on the composition of the plaque, with pathologists being able to characterize plaques that are at risk of rupture based on the plaque morphology. Typically, a vulnerable plaque (plaque prone to rupture) is characterized by increased macrophage infiltration and a thin fibrous cap [105]. Stable plaques are less inflammatory and have an increased smooth muscle cell and collagen content with a thicker fibrous cap. To assess plaque vulnerability, we adopted the formula for plaque vulnerability index (PVI) from established studies [106] (Fig. S9A). As demonstrated by ORO staining, DHA liposomes reduced the lipid accumulation in the plaques of the treated mice when compared to control liposomes-treated mice which were not effective (Fig. 8A & 8B). Additionally, infiltration of macrophages occurred to a lesser extent in the case of the DHA liposomes-treated mice (Fig. 8A & 8C). In terms of collagen content, DHA liposomes increased collagen type I in the plaques by upregulating the gene expression of collagen I to a higher extent than control liposomes (Fig. 8A, 8D, & S9B). However, no significant difference was observed in the smooth muscle actin (aSMA) staining between DHA- or control liposomes-treated mice (Fig. S9C & S9D). Based on the formula in Fig. S9A, we attempted to quantify the effects of

DHA liposomes on plaque vulnerability. Given the effects of DHA liposomes on lipid accumulation, macrophage infiltration and collagen content, the treatment with DHA liposomes was associated with enhanced atherosclerotic plaque stability with a lower plaque vulnerability index (PVI decreased by about 40%) compared to treatment with control liposomes (Fig. 8E & 8F). Plaques with high PVI have been correlated with a higher risk for adverse cardiovascular events [107]. Intravenous administration of DHA liposomes may therefore represent an additional therapeutic strategy to mitigate the risks of secondary events in patients with CVD [108].

3.9. DHA liposomes decrease the number of pro-inflammatory M1 macrophages and increase the number of reparative M2 macrophages in the plaques

It has been reported that M1 macrophages aggravate atherosclerosis progression by stimulating inflammation, whereas M2 macrophages promote plaque regression and stability by reducing inflammation and promoting wound healing [109]. In this study, we demonstrated DHA liposomes can reduce the number of M1 macrophages and repolarise M1 macrophages towards the M2 phenotype *in vitro* (Fig. 4). We also quantified the number of M1 and M2 macrophages *in vivo* and assessed the M1/M2 ratio in the atherosclerotic plaques of the ApoE$^{-/-}$ mice at the end of the 8 weeks intervention study. DHA liposomes reduced the number of M1 macrophages and increased the number of M2
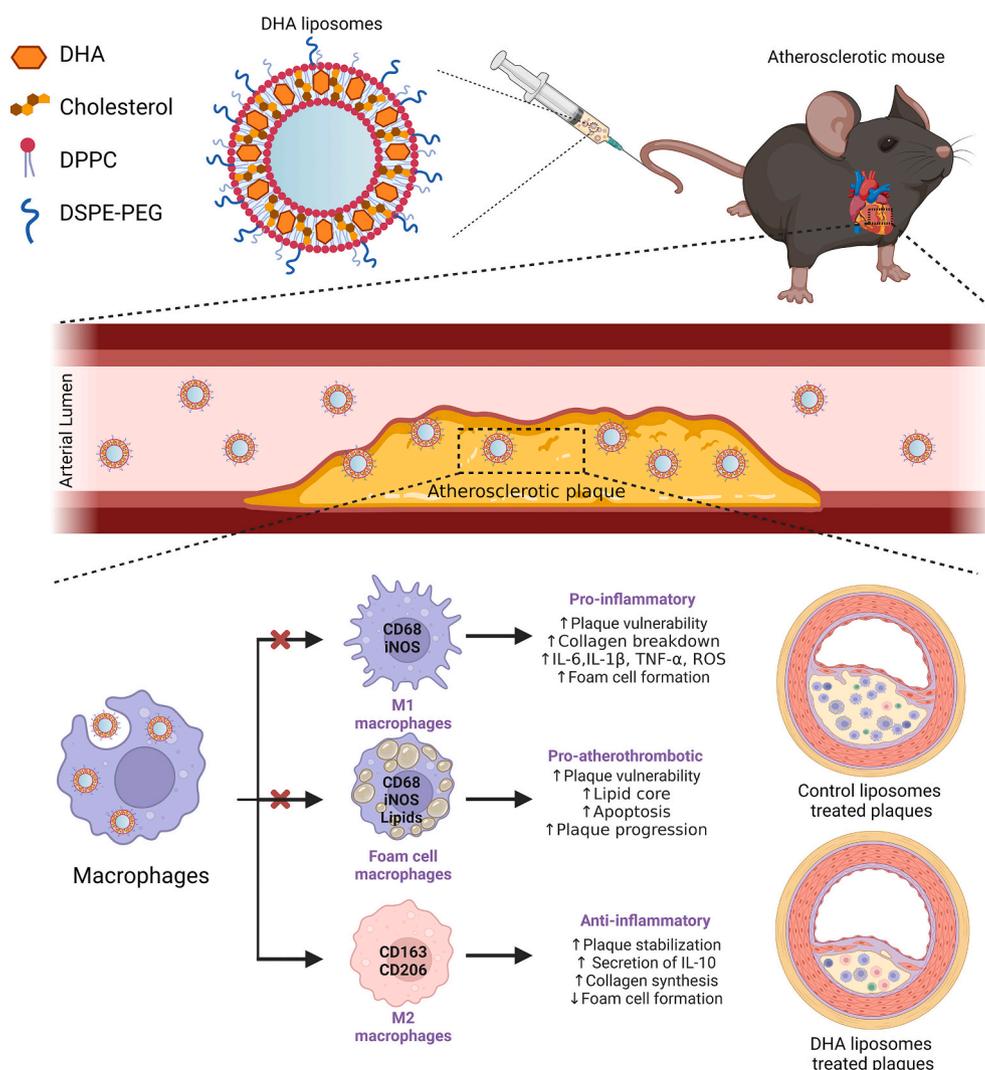
Fig. 10. Schematic illustration of atherosclerosis treatment with injectable liposomal DHA. Upon intravenous administration, DHA liposomes accumulate in the atherosclerotic plaques and are taken up by lesional macrophages. DHA liposomes inhibit inflammation by reducing pro-inflammatory M1 macrophages and increasing anti-inflammatory M2 macrophages within the plaques, suppress foam cell formation by inhibiting M1 macrophage uptake of oxidized LDL, and increase collagen production, thereby alleviating atherosclerosis progression and enhancing plaque stability.

macrophages (Fig. 9A, 9B, & 9C), resulting in lower ratios of M1/M2 macrophages (reduction by about 75%) in atherosclerotic plaques (Fig. 9D). Furthermore, DHA liposomes increased the gene expression of anti-inflammatory cytokine IL-10, the antioxidant enzyme SOD1, and M2 macrophage surface markers (CD163 and CD206) in the aorta wall compared to treatment with control liposomes (Fig. 9E – 9H). Interestingly, expression levels of the studied M2 surface markers are inversely associated with atherosclerosis progression in human patients [110]. It is important to note that M2 macrophages are abundant in stable atherosclerotic plaques in both human patients and animal models [110–112]. M2 macrophages may stabilize plaques and attenuate atherosclerosis progression by promoting collagen production and reducing foam cell formation [71,113] (Fig. 9I).

4. Conclusion

Liposomal encapsulation protects DHA from degradation while maintaining its bioactivity profile. Liposomes can direct the encapsulated DHA to macrophages in plaques of atherosclerotic mice resulting in anti-atherosclerotic activity *in vivo*. DHA liposomes inhibit inflammation, ROS production and OxLDL uptake-induced macrophage foam cell formation *in vitro*. Upon intravenous administration, DHA liposomes localize in atherosclerotic plaques and are taken up by lesional macrophages. As a result, DHA liposomes reduce atherosclerotic plaques and enhance plaque stability by decreasing macrophage infiltration, suppressing foam cell formation (lipid deposition), and increasing collagen content (Fig. 10). Furthermore, DHA liposomes increase the expression of anti-inflammatory IL-10 and promote polarization of plaque macrophages to the M2 phenotype. Our findings indicate that intravenous liposomal DHA represents a promising novel therapy to halt the progression of atherosclerosis and might find therapeutic application for the treatment of high-risk atherosclerosis patients. It might be interesting to evaluate the therapeutic effects of DHA liposomes *via* oral administration. However, since liposome integrity is damaged while going through the gastrointestinal degrading environment, resulting in aggregation and leakage of liposomes [114], one would expect that oral administration of the same dose of DHA liposomes as used for i.v. injections in the current study may yield very limited amount of DHA liposomes accessible to the atherosclerotic plaques (at least 40,000 to 400,000 times lower than reported therapeutic oral doses) and thus unlikely as effective in anti-atherosclerosis as i.v. administration. Nonetheless, to establish an acceptable dosing regimen which is suitable for intravenous treatment of patients, additional dose-response studies are mandatory.

CRediT authorship contribution statement

Suet Yen Chong: Data curation, Formal analysis, Investigation, Methodology, Writing – original draft, Writing – review & editing. **Xiaoyuan Wang:** Formal analysis, Investigation, Methodology. **Louis van Bloois:** Methodology, Resources. **Chenyuan Huang:** Formal analysis, Methodology, Resources, Visualization, Writing – review & editing. **Nilofer Sayed Syeda:** Investigation, Methodology. **Sitong Zhang:** Investigation, Methodology. **Hui Jun Ting:** Investigation, Methodology. **Vaarsha Nair:** Formal analysis, Methodology, Data curation. **Yuanzhe Lin:** Data curation, Formal analysis, Methodology. **Charles Kang Liang Lou:** Data curation, Investigation, Methodology. **Ayca Altay Benetti:** Data curation, Formal analysis, Methodology. **Xiaodong Yu:** Investigation, Methodology, Writing – review & editing. **Nicole Jia Ying Lim:** Data curation, Methodology. **Michelle Siying Tan:** Data curation, Investigation, Methodology. **Hwee Ying Lim:** Data curation, Methodology. **Sheau Yng Lim:** Data curation, Methodology. **Chung Hwee Thiam:** Data curation, Methodology. **Wen Donq Looi:** Data curation, Formal analysis, Methodology. **Olga Zharkova:** Data curation, Formal analysis, Methodology. **Nicholas W.S. Chew:** Data curation, Methodology. **Cheng Han Ng:** Formal analysis, Investigation, Methodology. **Glenn Kunnath Bonney:** Data curation, Methodology, Writing – review

& editing. **Mark Muthiah:** Formal analysis, Writing – review & editing. **Xiaoyuan Chen:** Formal analysis, Resources, Writing – review & editing. **Giorgia Pastorin:** Resources, Writing – review & editing. **A. Mark Richards:** Resources, Writing – review & editing. **Veronique Angeli:** Methodology, Writing – review & editing. **Gert Storm:** Formal analysis, Funding acquisition, Investigation, Writing – review & editing. **Jiong-Wei Wang:** Conceptualization, Data curation, Formal analysis, Funding acquisition, Investigation, Project administration, Resources, Supervision, Writing – original draft, Writing – review & editing.

Declaration of Competing Interest

There is no conflict of interest between the authors.

Data availability

Data will be made available on request.

Acknowledgements

Appendix A. Supplementary data

Supplementary data to this article can be found online at https://doi.org/10.1016/j.jconrel.2023.06.035.

References

[1] WHO Fact Sheets-CVDs. https://www.who.int/news-room/fact-sheets/detail/cardiovascular-diseases-(cvds), 2021 (accessed May 30, 2022).

[2] K. Sakakura, M. Nakano, F. Otsuka, E. Ladich, F.D. Kolodgie, R. Virmani, Pathophysiology of atherosclerosis plaque progression, Heart. Lung Circ. 22 (2013) 399–411, https://doi.org/10.1016/J.HLC.2013.03.001.

[3] P. Libby, P.M. Ridker, A. Maseri, Inflammation and atherosclerosis, Circulation. 105 (2002) 1135–1143, https://doi.org/10.1161/HC0902.104353.

[4] P. Libby, P.M. Ridker, Inflammation and Atherothrombosis: from population biology and bench research to clinical practice, J. Am. Coll. Cardiol. 48 (2006), https://doi.org/10.1016/J.JACC.2006.08.011.

[5] M. Naghavi, P. Libby, E. Falk, S.W. Casscells, S. Litovsky, J. Rumberger, J. J. Badimon, C. Stefanadis, P. Moreno, G. Pasterkamp, Z. Fayad, P.H. Stone, S. Waxman, P. Raggi, M. Madjid, A. Zarrabi, A. Burke, C. Yuan, P.J. Fitzgerald, D. S. Siscovick, C.L. de Korte, M. Aikawa, K.E. Juhani Airaksinen, G. Assmann, C. R. Becker, J.H. Chesebro, A. Farb, Z.S. Galis, C. Jackson, I.-K. Jang, W. Koenig, R. A. Lodder, K. March, J. Demirovic, M. Navab, S.G. Priori, M.D. Rekhter, R. Bahr, S.M. Grundy, R. Mehran, A. Colombo, E. Boerwinkle, C. Ballantyne, W. Insull, R. S. Schwartz, R. Vogel, P.W. Serruys, G.K. Hansson, D.P. Faxon, S. Kaul, H. Drexler, P. Greenland, J.E. Muller, R. Virmani, P.M. Ridker, D.P. Zipes, P. K. Shah, J.T. Willerson, From vulnerable plaque to vulnerable patient, Circulation vol. 108 (2003) 1664–1672, https://doi.org/10.1161/01.CIR.0000087480.94275.97.

[6] C.P. Cannon, E. Braunwald, C.H. McCabe, D.J. Rader, J.L. Rouleau, R. Belder, S. V. Joyal, K.A. Hill, M.A. Pfeffer, A.M. Skene, Intensive versus moderate lipid lowering with statins after acute coronary syndromes 350 (2004) 1495–1504, https://doi.org/10.1056/NEJMOA040583.

[7] C.P. Cannon, M.A. Blazing, R.P. Giugliano, A. McCagg, J.A. White, P. Theroux, H. Darius, B.S. Lewis, T.O. Ophuis, J.W. Jukema, G.M. De Ferrari, W. Ruzyllo, P. De Lucca, K. Im, E.A. Bohula, C. Reist, S.D. Wiviott, A.M. Tershakovec, T. A. Musliner, E. Braunwald, R.M. Califf, Ezetimibe added to statin therapy after acute coronary syndromes, N. Engl. J. Med. 372 (2015) 2387–2397, https://doi.org/10.1056/NEJMOA1410489/SUPPL_FILE/NEJMOA1410489_DISCLOSURES. PDF.

[8] P.M. Ridker, How common is residual inflammatory risk? Circ. Res. 120 (2017) 617–619, https://doi.org/10.1161/CIRCRESAHA.116.310527.

[9] P. Libby, K.E. Bornfeldt, A.R. Tall, Atherosclerosis: successes, surprises, and future challenges, Circ. Res. 118 (2016) 531–534, https://doi.org/10.1161/CIRCRESAHA.116.308334.

[10] P. Duewell, H. Kono, K.J. Rayner, C.M. Sirois, G. Vladimer, F.G. Bauernfeind, G. S. Abela, L. Franchi, G. Nüez, M. Schnurr, T. Espevik, E. Lien, K.A. Fitzgerald, K. L. Rock, K.J. Moore, S.D. Wright, V. Hornung, E. Latz, NLRP3 inflamasomes are required for atherogenesis and activated by cholesterol crystals that form early in disease, Nature. 464 (2010) 1357, https://doi.org/10.1038/NATURE08938.

[11] D. Karunakaran, M.A. Nguyen, M. Geoffrion, D. Vreeken, Z. Lister, H.S. Cheng, N. Otte, P. Essebier, H. Wyatt, J.W. Kandiah, R. Jung, F.J. Alenghat, A. Mompeon, R. Lee, C. Pan, E. Gordon, A. Rasheed, A.J. Lusis, P. Liu, L.P. Matic, U. Hedin, J. E. Fish, L. Guo, F. Kolodgie, R. Virmani, J.M. van Gils, K.J. Rayner, RIPK1 expression associates with inflammation in early atherosclerosis in humans and can be therapeutically silenced to reduce NF-κB activation and Atherogenesis in mice, Circulation. 143 (2021) 163–177, https://doi.org/10.1161/CIRCULATIONAHA.118.038379.

[12] P.M. Ridker, B.M. Everett, T. Thuren, J.G. MacFadyen, W.H. Chang, C. Ballantyne, F. Fonseca, J. Nicolau, W. Koenig, S.D. Anker, J.J.P. Kastelein, J. H. Cornel, P. Pais, D. Pella, J. Genest, R. Cifkova, A. Lorenzatti, T. Forster, Z. Kobalava, L. Vida-Simiti, M. Flather, H. Shimokawa, H. Ogawa, M. Dellborg, P. R.F. Rossi, R.P.T. Troquay, P. Libby, R.J. Glynn, Antiinflammatory therapy with Canakinumab for atherosclerotic disease, N. Engl. J. Med. 377 (2017) 1119–1131, https://doi.org/10.1056/NEJMOA1707914/SUPPL_FILE/NEJMOA1707914_DISCLOSURES.PDF.

[13] J.-C. Tardif, S. Kouz, D.D. Waters, O.F. Bertrand, R. Diaz, A.P. Maggioni, F. J. Pinto, R. Ibrahim, H. Gamra, G.S. Kiwan, C. Berry, J. López-Sendón, P. Ostadal, W. Koenig, D. Angoulvant, J.C. Grégoire, M.-A. Lavoie, M.-P. Dubé, D. Rhainds, M. Provencher, L. Blondeau, A. Orfanos, P.L. L'Allier, M.-C. Guertin, F. Roubille, Efficacy and safety of low-dose colchicine after myocardial infarction, N. Engl. J. Med. 381 (2019) 2497–2505, https://doi.org/10.1056/NEJMOA1912388/SUPPL_FILE/NEJMOA1912388_DATA-SHARING.PDF.

[14] N. Kromann, A. Green, Epidemiological studies in the Upernavik District, Greenland, Acta Med. Scand. 208 (1980) 401–406, https://doi.org/10.1111/J.0954-6820.1980.TB01221.X.

[15] R. Marchioli, Dietary supplementation with N-3 polyunsaturated fatty acids and vitamin E after myocardial infarction: results of the GISSI-Prevenzion trial, Lancet. 354 (1999) 447–455, https://doi.org/10.1016/S0140-6736(99)07072-5.

[16] D. Kromhout, E.B. Bosschieter, C.L. de Coulander, The inverse relation between fish consumption and 20-year mortality from coronary heart disease, N. Engl. J. Med. 312 (1985) 1205–1209, https://doi.org/10.1056/NEJM198505093121901.

[17] M. Artha, L.D. Aviglus, J. Eremiah, S. Tamler, N.J.O. Rencia, L.R.D. Yer, K. Iang, L. Iu, P. Hilip, G. Reenland, O.K.W. Alsh, D. Ouglas, M. Orris, B.S. Hekelle, Fish consumption and the 30-year risk of fatal myocardial infarction, N. Engl. J. Med. 336 (1997) 1046–1053, https://doi.org/10.1056/NEJM199704103361502.

[18] T.A. Dolecek, Epidemiological evidence of relationships between dietary polyunsaturated fatty acids and mortality in the multiple risk factor intervention trial (43413), Proc. Soc. Exp. Biol. Med. 200 (1992) 177–182, https://doi.org/10.3181/00379727-200-43413.

[19] P.C. Calder, J.A. Bond, D.J. Harvey, S. Gordon, E.A. Newsholme, Uptake and incorporation of saturated and unsaturated fatty acids into macrophage lipids and their effect upon macrophage adhesion and phagocytosis, Biochem. J. 269 (1990) 807–814, https://doi.org/10.1042/bj2690807.

[20] S. Shin, K. Jing, S. Jeong, N. Kim, K.S. Song, J.Y. Heo, J.H. Park, K.S. Seo, J. Han, J. Il Park, G.R. Kweon, S.K. Park, T. Wu, B.D. Hwang, K. Lim, The omega-3 polyunsaturated fatty acid DHA induces simultaneous apoptosis and autophagy via mitochondrial ROS-mediated Akt-mTOR signaling in prostate cancer cells expressing mutant p53, Biomed. Res. Int. 2013 (2013), https://doi.org/10.1155/2013/568671.

[21] M. Ali, K. Heyob, L.K. Rogers, DHA suppresses primary macrophage inflammatory responses via Notch 1/ Jagged 1 signaling, Sci. Report. 61 (6) (2016) 1–11, https://doi.org/10.1038/srep22276.

[22] A. Kishikawa, H. Kitaura, K. Kimura, S. Ogawa, J. Qi, W.R. Shen, F. Ohori, T. Noguchi, A. Marahleh, Y. Nara, A. Ichimura, I. Mizoguchi, Docosahexaenoic acid inhibits inflammation-induced osteoclast formation and bone resorption in vivo through GPR120 by inhibiting TNF-α production in macrophages and directly inhibiting osteoclast formation, Front. Endocrinol. (Lausanne). 10 (2019) 157, https://doi.org/10.3389/FENDO.2019.00157/BIBTEX.

[23] M.E. Clementi, G. Lazzarino, B. Sampaolese, A. Brancato, G. Tringali, DHA protects PC12 cells against oxidative stress and apoptotic signals through the activation of the NFE2L2/HO-1 axis, Int. J. Mol. Med. 43 (2019) 2523–2531, https://doi.org/10.3892/IJMM.2019.4170/DOWNLOAD.

[24] E. Dierge, E. Debock, C. Guilbaud, C. Corbet, E. Mignolet, L. Mignard, E. Bastien, C. Dessy, Y. Larondelle, O. Feron, Peroxidation of n-3 and n-6 polyunsaturated

[24] fatty acids in the acidic tumor environment leads to ferroptosis-mediated anticancer effects, Cell Metab. 33 (2021) 1701–1715.e5, https://doi.org/10.1016/J.CMET.2021.05.016.

[25] R. Kimura, N. Takahashi, S. Lin, T. Goto, K. Murota, R. Nakata, H. Inoue, T. Kawada, DHA attenuates postprandial hyperlipidemia via activating PPARα in intestinal epithelial cells, J. Lipid Res. 54 (2013) 3258–3268, https://doi.org/10.1194/JLR.M034942.

[26] A. Mansoori, G. Sotoudeh, M. Djalali, M.R. Eshraghian, M. Keramatipour, E. Nasli-Esfahani, F. Shidfar, E. Alvandi, O. Toupchian, F. Koohdani, Effect of DHA-rich fish oil on PPARγ target genes related to lipid metabolism in type 2 diabetes: a randomized, double-blind, placebo-controlled clinical trial, J. Clin. Lipidol. 9 (2015) 770–777, https://doi.org/10.1016/J.JACL.2015.08.007.

[27] A.C. Skulas-Ray, P.W.F. Wilson, W.S. Harris, E.A. Brinton, P.M. Kris-Etherton, C. K. Richter, T.A. Jacobson, M.B. Engler, M. Miller, J.G. Robinson, C.B. Blum, D. Rodriguez-Leyva, S.D. De Ferranti, F.K. Welty, Omega-3 fatty acids for the management of hypertriglyceridemia: a science advisory from the American Heart Association, Circulation. 140 (2019) E673–E691, https://doi.org/10.1161/CIR.0000000000000709.

[28] S.M. Grundy, N.J. Stone, A.L. Bailey, C. Beam, K.K. Birtcher, R.S. Blumenthal, L. T. Braun, S. De Ferranti, J. Faiella-Tommasino, D.E. Forman, R. Goldberg, P. A. Heidenreich, M.A. Hlatky, D.W. Jones, D. Lloyd-Jones, N. Lopez-Pajares, C. E. Ndumele, C.E. Orringer, C.A. Peralta, J.J. Saseen, S.C. Smith, L. Sperling, S. S. Virani, J. Yeboah, AHA/ACC/AACVPR/AAPA/ABC/ACPM/ADA/AGS/APhA/ ASPC/NLA/PCNA guideline on the Management of Blood Cholesterol: a report of the American College of Cardiology/American Heart Association task force on clinical practice guidelines, Circulation. 139 (2019) (2018) E1082–E1143, https://doi.org/10.1161/CIR.0000000000000625.

[29] F. Mach, C. Baigent, A.L. Catapano, K.C. Koskinas, M. Casula, L. Badimon, M. J. Chapman, G.G. De Backer, V. Delgado, B.A. Ference, I.M. Graham, A. Halliday, U. Landmesser, B. Mihaylova, T.R. Pedersen, G. Riccardi, D.J. Richter, M. S. Sabatine, M.R. Taskinen, L. Tokgozoglu, O. Wiklund, C. Mueller, H. Drexel, V. Aboyans, A. Corsini, W. Doehner, M. Farnier, B. Gigante, M. Kayikcioglu, G. Krstacic, E. Lambrinou, B.S. Lewis, J. Masip, P. Moulin, S. Petersen, A. S. Petronio, M.F. Piepoli, X. Pinto, L. Raber, K.K. Ray, Z. Reiner, W.F. Riesen, M. Roffi, J.P. Schmid, E. Shlyakhto, I.A. Simpson, E. Stroes, I. Sudano, A. D. Tselepis, M. Viigimaa, C. Vindis, A. Vonbank, M. Vrablik, M. Vrsalovic, J.L. Z. Gomez, J.P. Collet, S. Windecker, V. Dean, D. Fitzsimons, C.P. Gale, D. E. Grobbee, S. Halvorsen, G. Hindricks, B. Iung, P. Jüni, H.A. Katus, C. Leclercq, M. Lettino, B. Merkely, M. Sousa-Uva, R.M. Touyz, D. Nibouche, P.H. Zelveian, P. Siostrzonek, R. Najafov, P. Van De Borne, B. Pojskic, A. Postadzhiyan, L. Kypris, J. Spinar, M.L. Larsen, H.S. Eldin, T.E. Strandberg, J. Ferrières, R. Agladze, U. Laufs, L. Rallidis, L. Bajnok, T. Gudjonsson, V. Maher, Y. Henkin, M.M. Gulizia, A. Mussagaliyeva, G. Bajraktari, A. Kerimkulova, G. Latkovskis, O. Hamoui, R. Slapikas, L. Visser, P. Dingli, V. Ivanov, A. Boskovic, M. Nazzi, F. Visseren, I. Mitevska, K. Retterstøl, P. Jankowski, R. Fontes-Carvalho, D. Gaita, M. Ezhov, M. Foscoli, V. Giga, D. Pella, Z. Fras, L.P. De Isla, E. Hagström, R. Lehmann, L. Abid, O. Ozdogan, O. Mitchenko, R.S. Patel, ESC/EAS guidelines for the management of dyslipidaemias: lipid modification to reduce cardiovascular riskThe task force for the management of dyslipidaemias of the European Society of Cardiology (ESC) and European atherosclerosis society (EAS), Eur. Heart J. 41 (2020) (2019) 111–188, https://doi.org/10.1093/EURHEARTJ/EHZ455.

[30] X. Fei Guo, W. Feng Tong, Y. Ruan, A.J. Sinclair, D. Li, Different metabolism of EPA, DPA and DHA in humans: a double-blind cross-over study, Prostaglandins Leukot. Essent. Fat. Acids 158 (2020), https://doi.org/10.1016/j.plefa.2019.102033.

[31] J.A. Williams, S.E. Batten, M. Harris, B.D. Rockett, S.R. Shaikh, W. Stillwell, S. R. Wassall, Docosahexaenoic and eicosapentaenoic acids segregate differently between raft and nonraft domains, Biophys. J. 103 (2012) 228–237, https://doi.org/10.1016/j.bpj.2012.06.016.

[32] D.J. Manual Kollareth, R.J. Deckelbaum, Z. Liu, R. Ramakrishnan, C. Jouvene, C. N. Serhan, V.S. Ten, H. Zirpoli, Acute injection of a DHA triglyceride emulsion after hypoxic-ischemic brain injury in mice increases both DHA and EPA levels in blood and brain, Prostaglandins Leukot. Essent. Fat. Acids 162 (2020) 102176, https://doi.org/10.1016/J.PLEFA.2020.102176.

[33] A.H. Metherel, R.J.S. Lacombe, J.J. Aristizabal Henao, D. Morin-Rivron, A. P. Kitson, K.E. Hopperton, D. Chalil, M. Masoodi, K.D. Stark, R.P. Bazinet, Two weeks of docosahexaenoic acid (DHA) supplementation increases synthesis-secretion kinetics of n-3 polyunsaturated fatty acids compared to 8 weeks of DHA supplementation, J. Nutr. Biochem. 60 (2018) 24–34, https://doi.org/10.1016/J.JNUTBIO.2018.07.002.

[34] A.H. Metherel, M. Irfan, S.L. Klingel, D.M. Mutch, R.P. Bazinet, Compound-specific isotope analysis reveals no retroconversion of DHA to EPA but substantial conversion of EPA to DHA following supplementation: a randomized control trial, Am. J. Clin. Nutr. 110 (2019) 823–831, https://doi.org/10.1093/AJCN/NQZ097.

[35] A.H. Metherel, R. Chouinard-Watkins, M.O. Trépanier, R.J.S. Lacombe, R. P. Bazinet, Retroconversion is a minor contributor to increases in eicosapentaenoic acid following docosahexaenoic acid feeding as determined by compound specific isotope analysis in rat liver, Nutr. Metab. 14 (2017), https://doi.org/10.1186/S12986-017-0230-2.

[36] J. Brenna, DHA retroconversion revisited: dietary DHA spares endogenous EPA, Am. J. Clin. Nutr. 110 (2019) 789–790, https://doi.org/10.1093/AJCN/NQZ125.

[37] J. Allaire, W.S. Harris, C. Vors, A. Charest, J. Marin, K.H. Jackson, A. Tchernof, P. Couture, B. Lamarche, Supplementation with high-dose docosahexaenoic acid increases the Omega-3 index more than high-dose eicosapentaenoic acid,

prostaglandins, Leukot. Essent. Fat. Acids. 120 (2017) 8–14, https://doi.org/10.1016/J.PLEFA.2017.03.008.

[38] J.E. Manson, N.R. Cook, I.-M. Lee, W. Christen, S.S. Bassuk, S. Mora, H. Gibson, C. M. Albert, D. Gordon, T. Copeland, D. D'Agostino, G. Friedenberg, C. Ridge, V. Bubes, E.L. Giovannucci, W.C. Willett, J.E. Buring, Marine n−3 fatty acids and prevention of cardiovascular disease and cancer, N. Engl. J. Med. 380 (2019) 23–32, https://doi.org/10.1056/NEJMOA1811403/SUPPL_FILE/NEJMOA1811403_DATA-SHARING.PDF.

[39] S.J. Nicholls, A.M. Lincoff, M. Garcia, D. Bash, C.M. Ballantyne, P.J. Barter, M. H. Davidson, J.J.P. Kastelein, W. Koenig, D.K. McGuire, D. Mozaffarian, P. M. Ridker, K.K. Ray, B.G. Katona, A. Himmelmann, L.E. Loss, M. Rensfeldt, T. Lundström, R. Agrawal, V. Menon, K. Wolski, S.E. Nissen, Effect of high-dose Omega-3 fatty acids vs corn oil on major adverse cardiovascular events in patients at high cardiovascular risk: the STRENGTH randomized clinical trial, JAMA. 324 (2020) 2268–2280, https://doi.org/10.1001/JAMA.2020.22258.

[40] L.C. Del Gobbo, F. Imamura, S. Aslibekyan, M. Marklund, J.K. Virtanen, M. Wennberg, M.Y. Yakoob, S.E. Chiuve, L. Dela Cruz, A.C. Frazier-Wood, A. M. Fretts, E. Guallar, C. Matsumoto, K. Prem, T. Tanaka, J.H.Y. Wu, X. Zhou, C. Helmer, E. Ingelsson, J.M. Yuan, P. Barberger-Gateau, H. Campos, P.H. M. Chaves, L. Djoussé, G.G. Giles, J. Gómez-Aracena, A.M. Hodge, F.B. Hu, J. H. Jansson, I. Johansson, K.T. Khaw, W.P. Koh, R.N. Lemaitre, L. Lind, R. N. Luben, E.B. Rimm, U. Risérus, C. Samieri, P.W. Franks, D.S. Siscovick, M. Stampfer, L.M. Steffen, B.T. Steffen, M.Y. Tsai, R.M. Van Dam, S. Voutilainen, W.C. Willett, M. Woodward, D. Mozaffarian, ω-3 polyunsaturated fatty acid biomarkers and coronary heart disease: pooling project of 19 cohort studies, JAMA Intern. Med. 176 (2016) 1155–1166, https://doi.org/10.1001/JAMAINTERNMED.2016.2925.

[41] P. Sarajlic, G. Artiach, S.C. Larsson, M. Bäck, Dose-dependent risk reduction for myocardial infarction with Eicosapentaenoic acid: a meta-analysis and meta-regression including the STRENGTH trial, Cardiovasc. Drugs Ther. 35 (2021) 1079–1081, https://doi.org/10.1007/S10557-021-07212-Z/FIGURES/1.

[42] C. Hristine, M.A. Lbert, H. Annia, C. Ampos, M. Eir, J.S. Tampfer, A.M.R. Idker, O. A. Nn, E.M. Anson, W. Alter, C.W. Illett, Blood levels of long-chain n-3 fatty acids and the risk of sudden death, N. Engl. J. Med. 346 (2002) 1113–1118, https://doi.org/10.1056/NEJMOA012918.

[43] J. Dyerberg, P. Madsen, J.M. Møller, I. Aardestrup, E.B. Schmidt, Bioavailability of marine n-3 fatty acid formulations, Prostaglandins Leukot. Essent. Fat. Acids 83 (2010) 137–141, https://doi.org/10.1016/J.PLEFA.2010.06.007.

[44] B.B. Albert, D. Cameron-Smith, P.L. Hofman, W.S. Cutfield, Oxidation of marine Omega-3 supplements and human health, Biomed. Res. Int. 2013 (2013), https://doi.org/10.1155/2013/464921.

[45] K. Engstrm, A.S. Saldeen, B. Yang, J.L. Mehta, T. Saldeen, Effect of fish oils containing different amounts of EPA, DHA, and antioxidants on plasma and brain fatty acids and brain nitric oxide synthase activity in rats, Ups. J. Med. Sci. 114 (2009) 206–213, https://doi.org/10.3109/03009730903268958.

[46] A. Ismail, G. Bannenberg, H.B. Rice, E. Schutt, D. Mackay, Oxidation in EPA- and DHA-rich oils: an overview, Lipid Technol. 28 (2016) 55–59, https://doi.org/10.1002/LITE.201600013.

[47] M.O.W. Grimm, V.J. Haupenthal, J. Mett, C.P. Stahlmann, T. Blumel, N. T. Mylonas, K. Endres, H.S. Grimm, T. Hartmann, Oxidized docosahexaenoic acid species and lipid peroxidation products increase amyloidogenic amyloid precursor protein processing, Neurodegener. Dis. 16 (2016) 44–54, https://doi.org/10.1159/000440839.

[48] S. Judé, S. Bedut, S. Roger, M. Pinault, P. Champeroux, E. White, J.Y. Le Guennec, Peroxidation of docosahexaenoic acid is responsible for its effects on ITO and ISS in rat ventricular myocytes, Br. J. Pharmacol. 139 (2003) 816, https://doi.org/10.1038/SJ.BJP.0705308.

[49] B.B. Albert, J.G.B. Derraik, D. Cameron-Smith, P.L. Hofman, S. Tumanov, S. G. Villas-Boas, M.L. Garg, W.S. Cutfield, Fish oil supplements in New Zealand are highly oxidised and do not meet label content of n-3 PUFA, Sci. Report. 51 (5) (2015) 1–7, https://doi.org/10.1038/srep07928.

[50] S.A. Jackowski, A.Z. Alvi, A. Mirajkar, Z. Imani, Y. Gamalevych, N.A. Shaikh, G. Jackowski, Oxidation levels of north American over-the-counter n-3 (omega-3) supplements and the influence of supplement formulation and delivery form on evaluating oxidative safety, J. Nutr. Sci. 4 (2015) 10, https://doi.org/10.1017/JNS.2015.21.

[51] P.C. Calder, R.J. Deckelbaum, Intravenous fish oil in hospitalized adult patients: reviewing the reviews, Curr. Opin. Clin. Nutr. Metab. Care. 16 (2013) 119–123, https://doi.org/10.1097/MCO.0B013E32835DBDE9.

[52] D.J. Manual Kollareth, H. Zirpoli, V.S. Ten, R.J. Deckelbaum, Acute injection of Omega-3 triglyceride emulsion provides very similar protection as hypothermia in a neonatal mouse model of hypoxic-ischemic brain injury, Front. Neurol. 11 (2021), https://doi.org/10.3389/FNEUR.2020.618419.

[53] D.J. Manual Kollareth, R.J. Deckelbaum, Z. Liu, R. Ramakrishnan, C. Jouvene, C. N. Serhan, V.S. Ten, H. Zirpoli, Acute injection of a DHA triglyceride emulsion after hypoxic-ischemic brain injury in mice increases both DHA and EPA levels in blood and brain☆, prostaglandins, Leukot. Essent. Fatty Acids. 162 (2020), https://doi.org/10.1016/J.PLEFA.2020.102176.

[54] H. Zirpoli, M. Abdillahi, N. Quadri, R. Ananthakrishnan, L. Wang, R. Rosario, Z. Zhu, R.J. Deckelbaum, R. Ramasamy, Acute administration of n-3 rich triglyceride emulsions provides cardioprotection in murine models after ischemia-reperfusion, PLoS One 10 (2015), https://doi.org/10.1371/JOURNAL.PONE.0116274.

[55] I.E. Allijn, B.M.S. Czarny, X. Wang, S.Y. Chong, M. Weiler, A.E. da Silva, J. M. Metselaar, C.S.P. Lam, G. Pastorin, D.P.V. de Kleijn, G. Storm, J.-W. Wang, R. M. Schiffelers, Liposome encapsulated berberine treatment attenuates cardiac dysfunction after myocardial infarction, J. Control. Release 247 (2017) 127–133, https://doi.org/10.1016/j.jconrel.2016.12.042.

[56] F.M. van der Valk, D.F. van Wijk, M.E. Lobatto, H.J. Verberne, G. Storm, M.C. M. Willems, D.A. Legemate, A.J. Nederveen, C. Calcagno, V. Mani, S. Ramachandran, M.P.M. Paridaans, M.J. Otten, G.M. Dallinga-Thie, Z.A. Fayad, M. Nieuwdorp, D.M. Schulte, J.M. Metselaar, W.J.M. Mulder, E.S. Stroes, Prednisolone-containing liposomes accumulate in human atherosclerotic macrophages upon intravenous administration, Nanomedicine. 11 (2015) 1039, https://doi.org/10.1016/J.NANO.2015.02.021.

[57] M.E. Lobatto, V. Fuster, Z.A. Fayad, W.J.M.M. Mulder, Perspectives and opportunities for nanomedicine in the management of atherosclerosis, Nat. Rev. Drug Discov. 10 (2011) 835, https://doi.org/10.1038/NRD3578.

[58] A. Alaarg, N.Y. Jordan, J.J.F. Verhoef, J.M. Metselaar, G. Storm, R.J. Kok, Docosahexaenoic acid liposomes for targeting chronic inflammatory diseases and cancer: an in vitro assessment, Dove Press (2016), https://doi.org/10.2147/IJN.S115995.

[59] J.-W.W. Wang, M.S.C.C. Fontes, X. Wang, S.Y. Chong, E.L. Kessler, Y.-N.N. Zhang, J.J. de Haan, F. Arslan, S.C.A.A. de Jager, L. Timmers, T.A.B.B. Van Veen, C.S.P. Lam, D.P.V.D.V. de Kleijn, Leukocytic toll-like receptor 2 deficiency preserves cardiac function and reduces fibrosis in sustained pressure overload, Sci. Rep. 7 (2017) 9193, https://doi.org/10.1038/s41598-017-09451-3.

[60] D.P.V. de Kleijn, S.Y. Chong, X. Wang, S.M.J.M. Yatim, A.-M. Fairhurst, F. Vernooij, O. Zharkova, M.Y. Chan, R.S.Y. Foo, L. Timmers, C.S.P. Lam, J.-W. Wang, Toll-like receptor 7 deficiency promotes survival and reduces adverse left ventricular remodelling after myocardial infarction, Cardiovasc. Res. (2019), https://doi.org/10.1093/cvr/cvz057.

[61] S.Y. Chong, O. Zharkova, S.M.J.M. Yatim, X. Wang, X.C. Lim, C. Huang, C.Y. Tan, J. Jiang, L. Ye, M.S. Tan, V. Angeli, H.H. Versteeg, M. Dewerchin, P. Carmeliet, C. S.P. Lam, M.Y. Chan, D.P.V. De Kleijn, J.W. Wang, Tissue factor cytoplasmic domain exacerbates post-infarct left ventricular remodeling via orchestrating cardiac inflammation and angiogenesis, Theranostics. 11 (2021) 9243–9261, https://doi.org/10.7150/THNO.63354.

[62] C.Y.J. Lau, N. Benne, B. Lou, O. Zharkova, H.J. Ting, D. ter Braake, N. van Kronenburg, M.H. Fens, F. Broere, W.E. Hennink, J.-W. Wang, E. Mastrobattista, Modulating albumin-mediated transport of peptide-drug conjugates for antigen-specific Treg induction, J. Control. Release 348 (2022) 938–950, https://doi.org/10.1016/J.JCONREL.2022.06.025.

[63] V. Fournier, F. Destaillats, P. Juanéda, F. Dionisi, P. Lambelet, J.L. Sébédio, O. Berdeaux, Thermal degradation of long-chain polyunsaturated fatty acids during deodorization of fish oil, Eur. J. Lipid Sci. Technol. 108 (2006) 33–42, https://doi.org/10.1002/EJLT.200500290.

[64] S.W. Wong, M.J. Kwon, A.M.K. Choi, H.P. Kim, K. Nakahira, D.H. Hwang, Fatty acids modulate toll-like receptor 4 activation through regulation of receptor dimerization and recruitment into lipid rafts in a reactive oxygen species-dependent manner, J. Biol. Chem. 284 (2009) 27384–27392, https://doi.org/10.1074/jbc.m109.044065.

[65] W. Kong, J.H. Yen, E. Vassiliou, S. Adhikary, M.G. Toscano, D. Ganea, Docosahexaenoic acid prevents dendritic cell maturation and in vitro and in vivo expression of the IL-12 cytokine family, Lipids Health Dis. 9 (2010) 1–10, https://doi.org/10.1186/1476-511X-9-12/FIGURES/7.

[66] G. Li, Y. Li, B. Xiao, D. Cui, Y. Lin, J. Zeng, J. Li, M.J. Cao, J. Liu, Antioxidant activity of docosahexaenoic acid (DHA) and its regulatory roles in mitochondria, J. Agric. Food Chem. 69 (2021) 1647–1655, https://doi.org/10.1021/ACS.JAFC.0C07751/SUPPL_FILE/JF0C07751_SI_001.PDF.

[67] A.K. Bauer, L.D. Dwyer-Nield, J.A. Hankin, R.C. Murphy, A.M. Malkinson, The lung tumor promoter, butylated hydroxytoluene (BHT), causes chronic inflammation in promotion-sensitive BALB/cByJ mice but not in promotion-resistant CXB4 mice, Toxicology. 169 (2001) 1–15, https://doi.org/10.1016/S0300-483X(01)00475-9.

[68] R. Kahl, H. Kappus, Toxicology of the synthetic antioxidants BHA and BHT in comparison with the natural antioxidant vitamin E, Z. Lebensm. Unters. Forsch. 196 (1993) 329–338, https://doi.org/10.1007/BF01197931.

[69] C.O. Soulage, C.C. Pelletier, N. Florens, S. Lemoine, L. Dubourg, L. Juillard, F. Guebre-Egziabher, Two toxic lipid aldehydes, 4-hydroxy-2-hexenal (4-HHE) and 4-hydroxy-2-nonenal (4-HNE), accumulate in patients with chronic kidney disease, Toxins (Basel). 12 (2020), https://doi.org/10.3390/TOXINS12090567.

[70] O. Journal, L. Tao, Advances in food technology and nutritional sciences oxidation of polyunsaturated fatty acids and its impact on Food quality and human health article history, Adv. Food Technol. Nutr. Sci. Open J. 1 (2015) 135–142, https://doi.org/10.17140/AFTNSOJ-1-123.

[71] K.J. Moore, F.J. Sheedy, E.A. Fisher, Macrophages in atherosclerosis: a dynamic balance, Nat. Rev. Immunol. 13 (2013) 709, https://doi.org/10.1038/NRI3520.

[72] M.I. Cybulsky, C. Cheong, C.S. Robbins, Macrophages and dendritic cells: Partners in Atherogenesis, Circ. Res. 118 (2016) 637–652, https://doi.org/10.1161/CIRCRESAHA.115.306542.

[73] M.G. Sorci-Thomas, M.J. Thomas, Microdomains, inflammation, and atherosclerosis, Circ. Res. 118 (2016) 679–691, https://doi.org/10.1161/CIRCRESAHA.115.306246.

[74] C. Kelly, C. Jefferies, S.-A. Cryan, Targeted liposomal drug delivery to monocytes and macrophages, J. Drug Deliv. 2011 (2011) 1–11, https://doi.org/10.1155/2011/727241.

[75] V. Trouplin, N. Boucherit, L. Gorvel, F. Conti, G. Mottola, E. Ghigo, Bone marrow-derived macrophage production, J. Vis. Exp. (2013) 50966, https://doi.org/10.3791/50966.

[76] K.A. Binnemars-Postma, H.W. Ten Hoopen, G. Storm, J. Prakash, Differential uptake of nanoparticles by human M1 and M2 polarized macrophages: protein

corona as a critical determinant, Nanomedicine (London) 11 (2016) 2889–2902, https://doi.org/10.2217/NNM-2016-0233.

[77] K.M. Holmström, T. Finkel, Cellular mechanisms and physiological consequences of redox-dependent signalling, Nat. Rev. Mol. Cell Biol. 156 (15) (2014) 411–421, https://doi.org/10.1038/nrm3801.

[78] A.J. Kattoor, N.V.K. Pothineni, D. Palagiri, J.L. Mehta, Oxidative stress in atherosclerosis, Curr. Atheroscler. Rep. 19 (2017), https://doi.org/10.1007/S11883-017-0678-6.

[79] Z. Zhang, R. Dalan, Z. Hu, J. Wang, N.W. Chew, K. Poh, R. Tan, T.W. Soong, Y. Dai, L. Ye, X. Chen, Reactive oxygen species scavenging nanomedicine for the treatment of ischemic heart disease, Adv. Mater. (2022) 2202169, https://doi.org/10.1002/ADMA.202202169.

[80] A.P. West, I.E. Brodsky, C. Rahner, D.K. Woo, H. Erdjument-Bromage, P. Tempst, M.C. Walsh, Y. Choi, G.S. Shadel, S. Ghosh, TLR signalling augments macrophage bactericidal activity through mitochondrial ROS, Nature. 472 (2011) 476–480, https://doi.org/10.1038/NATURE09973.

[81] M.C. Basil, B.D. Levy, Specialized pro-resolving mediators: endogenous regulators of infection and inflammation, Nat. Rev. Immunol. 161 (16) (2015) 51–67, https://doi.org/10.1038/nri.2015.4.

[82] E. Lutgens, D. Lievens, L. Beckers, E. Wijnands, O. Soehnlein, A. Zernecke, T. Seijkens, D. Engel, J. Cleutjens, A.M. Keller, S.H. Naik, L. Boon, H.A. Oufella, Z. Mallat, C.L. Ahonen, R.J. Noelle, M.P. De Winther, M.J. Daemen, E.A. Biessen, C. Weber, Deficient CD40-TRAF6 signaling in leukocytes prevents atherosclerosis by skewing the immune response toward an antiinflammatory profile, J. Exp. Med. 207 (2010) 391–404, https://doi.org/10.1084/JEM.20091293.

[83] O.A. Akinrinmade, S. Chetty, A.K. Daramola, M.U. Islam, T. Thepen, S. Barth, CD64: an attractive immunotherapeutic target for M1-type macrophage mediated chronic inflammatory diseases, Biomedicines. 5 (2017), https://doi.org/10.3390/BIOMEDICINES5030056.

[84] Y. Bi, J. Chen, F. Hu, J. Liu, M. Li, L. Zhao, M2 macrophages as a potential target for Antiatherosclerosis treatment, Neural Plast. 2019 (2019), https://doi.org/10.1155/2019/6724903.

[85] M. Bäck, A. Yurdagul, I. Tabas, K. Öörni, P.T. Kovanen, Inflammation and its resolution in atherosclerosis: mediators and therapeutic opportunities, Nat. Rev. Cardiol. 16 (2019) 389–406, https://doi.org/10.1038/S41569-019-0169-2.

[86] A. Pirillo, G.D. Norata, A.L. Catapano, LOX-1, OxLDL, and atherosclerosis, Mediat. Inflamm. 2013 (2013), https://doi.org/10.1155/2013/152786.

[87] S. Singh, A.S. Gautam, Upregulated LOX-1 receptor: key player of the pathogenesis of atherosclerosis, Curr. Atheroscler. Rep. 21 (2019), https://doi.org/10.1007/s11883-019-0801-y.

[88] K. Tian, Y. Xu, A. Sahebkar, S. Xu, CD36 in atherosclerosis: pathophysiological mechanisms and therapeutic implications, Curr. Atheroscler. Rep. 22 (2020), https://doi.org/10.1007/S11883-020-00870-8.

[89] D.A. Chistiakov, A.A. Melnichenko, V.A. Myasoedova, A.V. Grechko, A. N. Orekhov, Mechanisms of foam cell formation in atherosclerosis, J. Mol. Med. (Berl.) 95 (2017) 1153–1165, https://doi.org/10.1007/S00109-017-1575-8.

[90] M.Q. Liu, Z. Chen, L.X. Chen, Endoplasmic reticulum stress: a novel mechanism and therapeutic target for cardiovascular diseases, Acta Pharmacol. Sin. 374 (37) (2016) 425–443, https://doi.org/10.1038/aps.2015.145.

[91] N.D. Donahue, H. Acar, S. Wilhelm, Concepts of nanoparticle cellular uptake, intracellular trafficking, and kinetics in nanomedicine, Adv. Drug Deliv. Rev. 143 (2019) 68–96, https://doi.org/10.1016/j.addr.2019.04.008.

[92] G.S. Getz, C.A. Reardon, Do the Apoe−/− and Ldlr−/−mice yield the same insight on atherogenesis? Arterioscler. Thromb. Vasc. Biol. 36 (2016) 1734, https://doi.org/10.1161/ATVBAHA.116.306874.

[93] G.S. Getz, C.A. Reardon, Animal models of atherosclerosis, Anim. Model. Study Hum. Dis. Second Ed. 816 (2017) 205–217, https://doi.org/10.1016/B978-0-12-809468-6.00008-5.

[94] R. Sun, X. Wang, Y. Liu, M. Xia, Dietary supplementation with fish oil alters the expression levels of proteins governing mitochondrial dynamics and prevents high-fat diet-induced endothelial dysfunction, Br. J. Nutr. 112 (2014) 145–153, https://doi.org/10.1017/S0007114514000701.

[95] T. Yoshihara, K. Shimada, K. Fukao, E. Sai, Y. Sato-Okabayashi, R. Matsumori, T. Shiozawa, H. Alshahi, T. Miyazaki, N. Tada, H. Daida, Omega 3 polyunsaturated fatty acids suppress the development of aortic aneurysms through the inhibition of macrophage-mediated inflammation, Circ. J. 79 (2015) 1470–1478, https://doi.org/10.1253/CIRCJ.CJ-14-0471.

[96] L. Liu, Q. Hu, H. Wu, Y. Xue, L. Cai, M. Fang, Z. Liu, P. Yao, Y. Wu, Z. Gong, Protective role of n6/n3 PUFA supplementation with varying DHA/EPA ratios against atherosclerosis in mice, J. Nutr. Biochem. 32 (2016) 171–180, https://doi.org/10.1016/J.JNUTBIO.2016.02.010.

[97] A. Takashima, D. Fukuda, K. Tanaka, Y. Higashikuni, Y. Hirata, S. Nishimoto, S. Yagi, H. Yamada, T. Soeki, T. Wakatsuki, Y. Taketani, M. Shimabukuro, M. Sata, Combination of n-3 polyunsaturated fatty acids reduces atherogenesis in apolipoprotein E-deficient mice by inhibiting macrophage activation, Atherosclerosis. 254 (2016) 142–150, https://doi.org/10.1016/J.ATHEROSCLEROSIS.2016.10.002.

[98] M.A. Alfaidi, J. Chamberlain, A. Rothman, D. Crossman, M.C. Villa-Uriol, P. Hadoke, J. Wu, T. Schenkel, P.C. Evans, S.E. Francis, Dietary docosahexaenoic acid reduces Oscillatory Wall shear stress, atherosclerosis, and hypertension, most likely mediated via an IL-1-mediated mechanism, J. Am. Heart Assoc. 7 (2018), https://doi.org/10.1161/JAHA.118.008757.

[99] B. Fuchs, J. Schiller, Application of MALDI-TOF mass spectrometry in lipidomics, Eur. J. Lipid Sci. Technol. 111 (2009) 83–98, https://doi.org/10.1002/EJLT.200800223.

[100] L. Shen, T. Yamamoto, X.W. Tan, K. Ogata, E. Ando, E. Ozeki, E. Matsuura, Identification and visualization of oxidized lipids in atherosclerotic plaques by microscopic imaging mass spectrometry-based metabolomics, Atherosclerosis. 311 (2020) 1–12, https://doi.org/10.1016/J.ATHEROSCLEROSIS.2020.08.001.

[101] M. Visscher, A.M. Moerman, N. Slijkhuis, K. Van Gaalen, H.M.M. Van Beusekom, T.M. Luider, A.F.W. Van Der Steen, K. Van Der Heiden, G. Van Soest, Human carotid atherosclerotic plaque characterization by MALDI mass spectrometry imaging, Atherosclerosis. 315 (2020) e84–e85, https://doi.org/10.1016/j.atherosclerosis.2020.10.259.

[102] A.M. Moerman, M. Visscher, N. Slijkhuis, K. Van Gaalen, B. Heijs, T. Klein, P. C. Burgers, Y.B. De Rijke, H.M.M. Van Beusekom, T.M. Luider, H.J.M. Verhagen, A.F.W. Van Der Steen, F.J.H. Gijsen, K. Van Der Heiden, G. Van Soest, Lipid signature of advanced human carotid atherosclerosis assessed by mass spectrometry imaging, J. Lipid Res. 62 (2021), https://doi.org/10.1194/JLR.RA120000974.

[103] P. Khamehgir-Silz, S. Gerbig, N. Volk, S. Schulz, B. Spengler, M. Hecker, A. H. Wagner, Comparative lipid profiling of murine and human atherosclerotic plaques using high-resolution MALDI MSI, Pflugers Arch. - Eur. J. Physiol. 474 (2022) 231–242, https://doi.org/10.1007/S00424-021-02643-X/FIGURES/5.

[104] K.J. Woollard, F. Geissmann, Monocytes in atherosclerosis: subsets and functions, Nat. Rev. Cardiol. 7 (2010) 77–86, https://doi.org/10.1038/NRCARDIO.2009.228.

[105] A. Lafont, Basic aspects of plaque vulnerability, Heart. 89 (2003) 1262, https://doi.org/10.1136/HEART.89.10.1262.

[106] M.D. Rekhter, How to evaluate plaque vulnerability in animal models of atherosclerosis? Cardiovasc. Res. 54 (2002) 36–41, https://doi.org/10.1016/S0008-6363(01)00537-5/2/54-1-36-GR2.GIF.

[107] I. Goncalves, J. Sun, C. Tengryd, M. Nitulescu, A.F. Persson, J. Nilsson, A. Edsfeldt, Plaque vulnerability index predicts cardiovascular events: a histological study of an endarterectomy cohort, J. Am. Heart Assoc. 10 (2021) 21038, https://doi.org/10.1161/JAHA.120.021038.

[108] S.D. Reilly, S.H. Litovsky, M.P. Steinkampf, J.B. Caulfield, Statins improve human coronary atherosclerotic plaque morphology, Texas Hear. Inst. J. 35 (2008) 99./pmc/articles/PMC2435445/ (accessed August 25, 2022).

[109] S. Colin, G. Chinetti-Gbaguidi, B. Staels, Macrophage phenotypes in atherosclerosis, Immunol. Rev. 262 (2014) 153–166, https://doi.org/10.1111/IMR.12218.

[110] M. de Gaetano, D. Crean, M. Barry, O. Belton, M1- and M2-type macrophage responses are predictive of adverse outcomes in human atherosclerosis, Front. Immunol. 7 (2016) 275, https://doi.org/10.3389/FIMMU.2016.00275/BIBTEX.

[111] K. Rahman, Y. Vengrenyuk, S.A. Ramsey, N.R. Vila, N.M. Girgis, J. Liu, V. Gusarova, J. Gromada, A. Weinstock, K.J. Moore, P. Loke, E.A. Fisher, Inflammatory Ly6Chi monocytes and their conversion to M2 macrophages drive atherosclerosis regression, J. Clin. Invest. 127 (2017) 2904–2915, https://doi.org/10.1172/JCI75005.

[112] J.E. Feig, J. Parathath, J.X. Rong, S.L. Mick, Y. Vengrenyuk, L. Grauer, S. G. Young, E.A. Fisher, Reversal of hyperlipidemia with a genetic switch favorably affects the content and inflammatory state of macrophages in atherosclerotic plaques, Circulation. 123 (2011) 989–998, https://doi.org/10.1161/CIRCULATIONAHA.110.984146.

[113] T.J. Barrett, Macrophages in atherosclerosis regression, Arterioscler. Thromb. Vasc. Biol. 40 (2020) 20–33, https://doi.org/10.1161/ATVBAHA.119.312802.

[114] L. Tong, S. Zhang, Q. Liu, C. Huang, H. Hao, M.S. Tan, X. Yu, C.K.L. Lou, R. Huang, Z. Zhang, T. Liu, P. Gong, C.H. Ng, M. Muthiah, G. Pastorin, M. G. Wacker, X. Chen, G. Storm, C.N. Lee, L. Zhang, H. Yi, J.W. Wang, Milk-derived extracellular vesicles protect intestinal barrier integrity in the gut-liver axis, Sci. Adv. 9 (2023) eade5041, https://doi.org/10.1126/SCIADV.ADE5041.